Study of Satellite Derived Aerosol Properties and Validation with Ground-Truth Data

A thesis submitted to

Gujarat University

for the degree of

Doctor of Philosophy in Physics

by

Amit Misra

Space and Atmospheric Science Division
Physical Research Laboratory
Ahmedabad 380009 India

April, 2008

CERTIFICATE

I hereby declare that the work presented in this thesis is original and has not formed the basis for the award of any degree or diploma by any university or institution.

Amit Misra
(Author)

Certified by:

Prof. A. Jayaraman
(Thesis Supervisor)
Space and Atmospheric Science Division
Physical Research Laboratory
Ahmedabad, 380009 (India)

To Gãyatrĩ

Contents

Acknowledgements

First and foremost I want to thank my supervisor Prof A. Jayaraman whose guidance has culminated into this thesis. It has been a great pleasure to be associated with him for such a long time. I deeply appreciate his patience and understanding as well as the enthusiasm he generates making association with him a fantastic experience.

I want to express my deepest gratitude to Prof Shyam Lal for his encouragement and support related to academic as well as administrative affairs. It was an honour for me to be taught the basics of atmospheric sciences by him during the course work and in fact it was the enthusiasm generated in his classes which motivated me to join this division.

I also want to thank Dr Ramachandran for various discussions related to aerosols and radiative transfer through which I gained a lot of insight and understanding of the subject.

I gained a lot of academic knowledge, guidance and sage advice from my seniors Lokesh, Harish and Dilip which helped me overcome several problems of academic and non-academic nature. Harish in particular deserves special mention since he is the person who introduced me to IDL in which some of the codes used in the present work are written. I extend my deepest appreciation to the love and support I have received from them. Sanat and Sumita with their various questions about aerosols, radiative transfer and remote sensing helped me refresh my learning. I want to thank them for all their discussions and for making the ambience lively by their presence. I want to make special mention of Rajesh T. A. who extended technical support ever since the start of my research career. For me, he has always been the first person to seek whenever any problem comes up.

I express by gratitude and thanks to all the members of the Space and Atmospheric Science Division who have directly or indirectly helped me in my academic work. I extend my deep regards to members of the Library, Computer Centre and Administration Section for providing support in their respective areas and making the working environment as much comfortable as possible.

I acknowledge Robert C. Levy (University of Maryland), Michael D. King and N. Christina Hsu (NASA-GSFC) for providing details, updates and clarifications regarding MODIS aerosol product. I also acknowledge LPDAAC for providing the MODIS aerosol product data used in this study. Studies on Delhi and peninsular India were carried out as part of the ISRO-GBP Land Campaigns I and II. I want to acknowledge the ISRO programme office for the support provided.

I apologize to my parents and sisters for having deprived them of the time which they deserved and deeply appreciate their patience and understanding. Hopefully I will be able to spend more time with them now.

I have kept two names to mention in the end: Subimal and Subhasis. Subimal's expertise in handling any software developed under the sky and his enormous knowledge about anything from Dostoyevsky to Python Programming makes him the most sought after person in PRL. It was an honour for me to have him by my side whenever I needed him most. Besides providing computational, technical and data-handling support, Subhasis' presence made the most comfortable period during my whole 5 year tenure at Ahmedabad. These two are the biggest assets I gained during my tenure in Ahmedabad. Even though they were also the ones who gave me a lot of headache, I simply cannot imagine how life would had been without them. The gratitude to them cannot be expressed in words, I can only say: Thank you.

Amit

Chapter 1

Introduction

Aerosols are in the forefront of climate studies since last two decades owing to the role they play in the Earth-Atmosphere system by absorbing or scattering the incoming solar radiation thus warming or cooling the atmosphere [Bellouin et al., 2005]. Their optical properties which depend on their chemical composition, size and shape, determine their radiative behaviour which in turn determines the overall effect they will have on the Earth radiation budget [Charlson et al., 1992, Chung et al., 2005]. The major problem in their characterization is on account of their short lifetime because of which they have high spatial and temporal variability [Seinfeld and Pandis, 1997]. Besides, the transport processes may bring in aerosols from other locations and affect the local climate there. These factors reinforce the necessity of aerosol monitoring on a larger spatial scale than can be provided by the ground based measurements[*IPCC*, 2001].

Satellite based observations can provide detailed knowledge in this regard on a long time scale covering a large spatial area [Kaufman et al., 2002b]. They have an additional advantage, compared to conventional ground based observations, in that since the same instrument is making observation globally, the aerosol concentration at different locations can be compared which will not be affected by the calibration errors of the instrument. Since they don't interfere with the ambient aerosol composition, they provide the ideal remote sensing method. Satellite based remote sensing is also used to infer

aerosol climatology viz., details of global aerosol distribution and seasonal variation as well as sources and sinks of specific aerosol types. For example, spatial patterns in aerosol distribution can be inferred from polar satellites while temporal patterns can be obtained from geostationary satellites. Such information has further applications in atmospheric correction of satellite images to derive land products to study land use, land cover, surface reflectance and several other parameters. Aerosol monitoring from space based instruments consists in extracting the atmospheric contribution from the total signal measured by the satellite sensor. Aerosol monitoring from previous sensors, such as the AVHRR [Husar et al., 1997], was limited to studies over oceans which have a distinct advantage in that the total measured signal is not much affected by reflectance from ocean surface away from sun-glint area [King et al., 1999]. Besides AVHRR, aerosol characterization has been tried by TOMS over land and ocean but its accuracy is affected by the large footprint resulting in cloud contamination related problems [Torres et al., 1998]. Still, aerosol retrieval over oceans is more accurate and reliable. Studies over land are comparatively more challenging because of the large surface reflectance which may introduce considerable errors in the retrieved results.

The initial attempts for aerosol retrieval over land were made with the launch of the POLDER instrument [Deschamps et al., 1994] which utilised the information regarding the polarization state of the radiation for the purpose [Leroy et al., 1997] but had limitations with onboard calibration. It lasted for only 8 months due to technical problems in the spacecraft. Aerosol monitoring over land entered a new era with the launch of the MODIS instrument [Barnes et al., 1998] onboard the NASA satellites Terra and Aqua in 1999 and 2002 respectively. It measures the Earth leaving radiances in 36 high resolution bands from 0.4 to 14.0 microns with a spatial resolution of 250m, 500m and 1 km depending on the wavelength. Its large swath of 2330 km allows the nearly global coverage within 1 or 2 days. The major highlights of MODIS is the large number of spectral bands and excellent on-board calibration. MODIS includes several important characteristics and attributes of the previous sensors such as the Coastal Zone Colour Scanner (CZCS), Advanced Very High Resolution Radiometer (AVHRR), High Res-

olution Infrared Radiation Sounder (HIRS) and Landsat Thematic Mapper (TM). The large number of data products from MODIS are used for studying various land, ocean and atmosphere processes. The wide spectral coverage has advantage in deriving aerosol size distribution information and hence in uncoupling the total aerosol amount into contribution from natural and anthropogenic parts [Kaufman et al., 2005]. Parallel measurement in visible and IR channels has also helped in overcoming the biggest obstacle in the aerosol retrieval over land viz, the separation of the surface reflectance part from the total measured signal [King et al., 1992, 1999, 2003]. The primary parameter given by the MODIS aerosol product is the Aerosol Optical Depth (AOD) which is a measure of the columnar atmospheric aerosol content. Besides, MODIS also provides information regarding fine-mode fraction over land and ocean and effective radius over ocean. Such information is required in the study of Earth radiation balance and hydrological cycle to assess the aerosol impact on these processes [Chu and Remer, 2006]. Having same instrument on two platforms with different equatorial crossing times makes the study of diurnal variation in aerosol properties feasible. MODIS derived aerosol products are also used for air quality monitoring as well as in predicting future air quality [Hutchison, 2003, Hutchison et al., 2004]. It should be noted that using ground based observations to monitor air quality may provide incorrect information in case the pollution is transported from other regions [Hutchison, 2003]. One of the achievements of MODIS is the correlation between the aerosol optical depth and $PM_{2.5}$ mass concentration so that the aerosol product can be used as a tracer for $PM_{2.5}$ mass concentration thus providing better identification of pollution sources [Kafatos and Qu, 2006]. Besides the direct products, which themselves are useful in various studies as mentioned above, MODIS data has been used in conjunction with data from other sensor to arrive at several interesting results [Edwards et al., 2004].

In spite of these advantages, the space based aerosol measurements from MODIS, like any other sensor, suffer from various drawbacks. These include possibility of cloud contamination and errors arising due to various assumptions in the retrieval algorithm principally about the aerosol type and surface reflectance. To circumvent the uncertainties pertaining to these parameters,

the procedure relies on the ground based observations which provide the exhaustive database of the aerosol microphysical properties [D'Almeida et al., 1991, Holben et al., 1998]. Even after the retrieval has been accomplished, the satellite retrieved data has to be validated against the ground truth data. Being based on the measurement of attenuation in direct solar radiation, data from ground based observations are not limited by the aerosol type and surface reflectance related constraints. For example, during a particular day, several observations can be taken from sunphotometer so that any peculiar change in AOD due to possible cloud contamination can be identified and removed. This is not possible from single observation carried out by satellite sensor which has to rely on cloud screening tests. Further, sunphotometer measures the aerosol optical depth by measuring the attenuation in the direct solar radiation so that there is no need to have any knowledge regarding the aerosol type. But the retrieval of aerosol optical depth from satellite sensor is an inversion process based on the radiative transfer calculations for which the knowledge of aerosol model is essential. Hence, ground based observations represent the benchmark against which to verify the accuracy and validity of satellite based retrievals. An extensive validation exercise tests the efficacy of the retrieval algorithm, conditions under which it works satisfactorily and cases where further improvement is needed. Further, the validation exercise helps to quantify the improvements to the algorithm which are made from time to time. Validation of MODIS aerosol optical depth data started and is in progress nearly since the data from the sensor started coming in. Chu et al. [2002, 2003], Ichoku et al. [2002, 2003], Remer et al. [2002, 2005], Levy et al. [2005] and several other groups working on the validation efforts report their results based on the extensive validation of the aerosol product at its different stages of development. But a detailed and extensive validation of the MODIS Level 2 data over the Indian subcontinent was till recently lacking. For example, Tripathi et al. [2005] studied 1 year of Level 2 data whereas Jethva et al. [2005] and Prasad and Singh [2007] used Level 3 gridded data for their comparisons. More details on their results will be discussed in the Results and Discussion section. The present paper discusses the validation of 4 years of the Level 2 MODIS retrieved aerosol optical depth product over

Ahmedabad, an urban location in western India. All three versions of the aerosol product are considered so as to be able to assess the improvement in accuracy with transition from Collection Version 4 to version 5 and Deep Blue Algorithm. In the present study, the aerosol product data from both the Aqua as well as Terra platform is used. Further, to the best of our knowledge, this is the first time that the validation results of the Deep Blue Algorithm (included in the Aqua Collection Version C005 data) over India are being reported.

Chapter 2 titled *Satellite Algorithms* provides an overview of the MODIS retrieval algorithm for version 4 and upgrades to version 5. Further, the alternative retrieval scheme, known as the Deep Blue Algorithm, for aerosol retrieval over highly reflecting surfaces is also discussed. Here, only the algorithm over land is discussed. Chapter 3 on *Ahmedabad Meteorology* provides the details of local meteorology over Ahmedabad which is the study location for the validation of MODIS aerosol product using 4 years of ground based sunphotometer data to investigate temporal variations in the correlation parameters of the two sets of measurements. This is important while discussing the differences in the ground truth values and the MODIS retrieved values of the aerosol optical depth. Instrumentation details of MODIS and the various data products available alongwith the principle and working of the Microtops sunphotometer are discussed in Chapter 4 titled *Instruments*. This chapter also includes details of data analysis which is followed to process the satellite and ground based data for different validation exercises. Chapter 5- *Validation Results for Ahmedabad*- provides details of the validation results over Ahmedabad. The 4 years of data has been disaggregated into individual years and different seasons to identify the cases where the differences in the retrievals from MODIS and Microtops are maximum and minimum. In addition to the study of temporal variation in the correlation parameters from a fixed location, validation of MODIS aerosol product has also been carried out during the two ISRO-GBP Land Campaigns. The first Land Campaign was carried out in the peninsular India to characterize the distribution of aerosols over this region whereas the objective of second Land Campaign was the study of distribution of aerosol along the Indo-Gangetic plain and

its impact on fog formation. Validation results of MODIS derived AOD from these two experiments constitute Chapter 6 titled *Validation Results for the ISRO-GBP Land Campaigns*. Finally, all the results and inferences of the various studies are summarized in Chapter 7.

Chapter 2

Satellite Algorithms

The scheme for the retrieval of aerosol properties from the MODIS sensor has remained essentially the same as proposed by Kaufman et al. [1997a], though several modifications have been implemented from time to time based on the validation results by different groups all over the world under different environmental and geographical conditions which showed the exact cases where further modifications are needed. We first discuss the Kaufman et al. [1997a] algorithm and its operational version as implemented by Remer et al. [2005]. The latest overhaul to this algorithm which culminated in the C005 version of the MODIS algorithm [Levy et al., 2007b] is discussed next. Finally, the alternative procedure - the Deep Blue algorithm - for retrieval of aerosol properties over regions with high surface reflectance as proposed by Hsu et al. [2004] is discussed.

2.1 MODIS Aerosol Retrieval Algorithm: The Collection Version C004

The underlying principle behind the satellite based retrieval of aerosol properties is the radiative transfer equation [Vermote et al., 1997]:

$$\rho^*(\theta_0, \theta, \phi) = \rho_a(\theta_0, \theta, \phi) + \frac{\rho_s}{1 - \rho_s S} T(\theta_0) T(\theta) \tag{2.1}$$

where ρ^* is the apparent reflectance at the satellite level, θ_0 is the solar zenith angle, θ the satellite zenith angle and ϕ the relative azimuth angle. ρ^s is the surface reflectance and T is the total transmission function.

The atmospheric path radiance contribution itself is composed of the molecular and aerosol contributions. The contribution by aerosol is expressed in terms of single scattering albedo ω_0, aerosol optical depth τ_a and phase function P_a, so that:

$$\rho_a(\theta_0, \theta, \phi) \quad = \quad \rho_m(\theta_0, \theta, \phi) + \frac{\omega_0 \tau_a P_a}{4\mu\mu_0} \tag{2.2}$$

where $\rho_m(\theta_0, \theta, \phi)$ is the molecular path radiance, $\mu = \cos\theta$ and $\mu_0 = \cos\theta_0$. After the satellite measured signal has been corrected for the gaseous absorption, aerosol optical depth τ_a can be retrieved by inversion of the above equations, provided the aerosol properties ω_0 and P_a are known. Another obstacle is the surface reflectance which constitutes the biggest source of error in the retrieved results. The error in retrieved aerosol optical depth is 10 times the error in reflectance value.

To get around the problem of separating out the contribution of surface reflectance from the total measured signal measured by MODIS, the algorithm employs the Dark Target Approach. Dark targets are the pixels in the satellite image with surface reflectance lower than 0.15 e.g., forest covers, wet soils and vegetation etc. This also implies that the algorithm has drawback in that the aerosol optical depth cannot be retrieved over surfaces having reflectance values higher than this critical value. The basic motive for selecting the dark pixels for AOD retrievals is that the contribution from the atmosphere to the total measured signal is lower for shorter wavelengths and low surface reflectance so that the error in retrieved AOD is smaller.

Further, the error due to aerosol absorption properties is also low under these conditions. The overall procedure consists of first identifying the dark pixels in the image from the values of radiances in the mid-IR. This is illustrated in Figure 2.1 where images of the western Indian state of Gujarat from MODIS Level 1B geolocated radiance data are shown for three wavelengths-

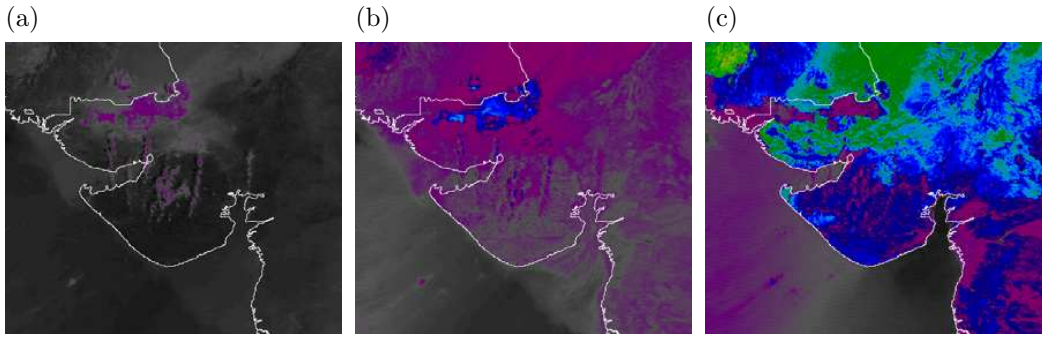

Figure 2.1: Radiance images of Gujarat from MODIS (a) channel 3 (470 nm), (b) channel 1 (660 nm) and (c) channel 5 (2130 nm). The 2130 nm image reveals surface features which are not discernable in the other two channels because of negligible contribution from the atmosphere in mid-IR.

470 nm, 660 nm and 2130 nm. Here we see the surface features revealed at 2130 nm which are not discernable at the two visible wavelengths. This is because the wavelength in mid-IR is fairly larger than the size of most of the aerosol species so that there is negligible contribution from atmosphere in the mid-IR. However, this may not hold good in the presence of dust. This principle has been applied to detect dark vegetation using the 3700 nm for remote sensing of aerosol over land (e.g., Holben et al. [1992], Kaufman and Remer [1994]). For application to MODIS algorithm, 2130 nm is used because in contrast to 3700 nm, 2130 nm is not affected by surface emission though it is affected by water absorption. Still, it is more reliable since correction for atmospheric absorption is more accurate than surface emission correction. At the next step, the surface reflectance of these pixels in the red and blue channels are derived from the corresponding values in the mid-IR using the empirical relations:

$$\begin{aligned} R_{470} &= \frac{R_{2130}}{4} \\ R_{660} &= \frac{R_{2130}}{2} \end{aligned} \tag{2.3}$$

These relations were derived based on the atmospheric correction of Land-

sat TM and AVIRIS images during SCAR-A (Sulphates Cloud and Radiation experiment- Atlantic) and take into account various types of surfaces such as forests, vegetation, soils and urban surface types.

Equations 2.3 represent parallel processes affecting the surface reflectance values in the visible and mid-IR. For example, vegetation, soil moisture content and shadows reduce the reflectance in both visible as well as the mid-IR wavelengths. In the case of vegetation, reflectance is lowered in the visible due to chlorophyll absorption whereas due to liquid water absorption in the mid-IR. Similarly, in the case of wet soil, water absorption reduces the reflectance in the mid-IR whereas in the visible wavelengths, the reflectance is reduced due to the light trapping mechanism [Kaufman et al., 1997b, 2002a]. After an estimate of surface reflectance has been made, satellite radiances are inverted to aerosol optical depth values using the continental aerosol model making use of Look-up tables which contain the pre-computed values of simulated TOA radiances as a function of surface reflectance, optical thickness and solar and satellite geometry. The minimum difference between the measured and simulated radiances represent the spectral aerosol optical depth.

This initial guess of the aerosol optical depth is used in conjunction with the radiance ratio in the red and blue channels and the geographical location of the region under consideration to arrive at the decision about the actual aerosol model. In this pre-launch algorithm, the initial guess of aerosol optical depth (retrieved using the continental aerosol model), is corrected based on the decision about the actual aerosol model. The predicted uncertainty in the retrieved aerosol optical depth from this algorithm is $\Delta\tau = \pm\ 0.05\ \pm 0.15\tau$. The major sources of error are uncertainties in the surface reflectance and aerosol model.

The methodology proposed by Kaufman et al. [1997a] was implemented in the MODIS operational algorithm [Remer et al., 2005] for remote sensing of aerosols with few modifications. The algorithm now allowed the upper limit of the surface reflectance to be 0.25 so that more brighter surfaces were incorporated and thus a larger geographical area was covered. In addition to the aerosol models used in the algorithm by Kaufman et al. [1997a], Re-

mer et al. [2005] included an additional aerosol model - the heavy absorption model- after validation by Ichoku et al. [2003] during SAFARI 2000 experiment showed need for increased light absorption over certain areas. Besides, the geographical distribution of aerosol models was also modified. Kaufman et al. [1997a] had proposed a correction to the initial estimate of the aerosol optical depth (derived using the continental model) after decision regarding the actual aerosol model is reached based on the path radiance ratio test and the geographical location of the study area. Remer et al. [2005] instead proposed a full retrieval after the decision on correct aerosol model is reached. In addition, an alternative approach was proposed to retrieve aerosol optical depth over highly reflecting surfaces using 470 nm and continental aerosol model due to less number of pixels over such surfaces remain after the filtering in the usual method. Since retrieval is made in a single wavelength, the path radiance technique cannot be used to reach the decision about the aerosol model so that AOD is reported only in a single channel and has less accuracy.

2.2 MODIS Aerosol Retrieval Algorithm: The Collection Version C005

The previous MODIS algorithm (Collection version C004) has recently been updated [Levy et al., 2007b] to improve its performance after the initial validation results showed scope for further improvement when compared with the ground based observations [Chu et al., 2002, 2003, Ichoku et al., 2002, 2003, Remer et al., 2005, Levy et al., 2005]. The modifications correspond to the inclusion of polarization in the radiative transfer calculation [Levy et al., 2004], the angular dependence of surface reflectance ratios [Remer et al., 2001, Gatebe et al., 2001]; and the update of the aerosol models based on the aerosol climatology derived from the worldwide AERONET observations [Dubovik et al., 2002].

Levy et al. [2004] discuss the effect of neglecting polarization in the radiative transfer calculations for the aerosol retrieval algorithm in the C004

version. Though the aerosol retrieval algorithm over oceans uses a vector radiative transfer code, that over land employs a scalar code [Dave, 1970] for the radiative transfer calculations. This is because Dave code is one of the most extensively used codes in the satellite remote sensing community and is the one which is best understood. Since previous sensors made retrievals in mainly the red and IR channels, polarisation was not considered an issue which has minimal effect at longer wavelength. But MODIS employs 470 nm wavelength also for the retrieval at which the optical depth is higher and therefore polarisation effects are also non-negligible. Though MODIS does not measure polarisation, its non-inclusion in the radiative transfer calculation may lead to erroneous estimates in the retrieved optical depths. Using a polarized radiative transfer code RT3 [Evans and Stephens, 1994], Levy et al. [2004] calculated the TOA reflectances for pre-defined set of solar and satellite geometries, atmospheric parameters and aerosol model with and without consideration of polarization effects. They found non-zero errors which were positive or negative depending on the scattering angle. The magnitude of error was determined by the specific solar and satellite geometry. The error was higher at blue as compared to red, viz. about double at higher optical depths and about eight times at smaller values of optical depth. This is in accordance to as postulated by Fraser and Stephens [1994] and is due to higher optical depths and corresponding multiple scattering effects at blue as compared to red. In addition, Levy et al. [2004] evaluated the related error in the retrieved aerosol optical depth corresponding to this error in the reflectance. In most of the cases, the error in retrieved optical depth is about 10 times the error in reflectance though for some particular geometries, it could be as high as 30 times. A positive error in reflectance due to neglect of polarisation results in a negative error in retrieved aerosol optical depth. If for a given aerosol optical depth, the reflectance in the presence of polarisation is higher than the scalar case, then the aerosol optical depth corresponding to the input reflectance must be lower than the scalar AOD value. However, these errors get cancelled out while evaluating long-term and global averages so that the aerosol climatology as derived without taking polarization into account is not affected. The updated version 5 uses

the radiative transfer code RT3 [Evans and Stephens, 1994] for the purpose which performs the radiative transfer calculations taking polarization into account. The aerosol optical properties required by RT3 are calculated using the MieV code [Wiscombe, 1994].

The empirical relations in Equation 2.3 were derived for nadir-looking observations from the Landsat TM and AVIRIS data so that any angular or seasonal dependence of these ratios will not be reflected here. Remer et al. [2001] studied the angular and seasonal variations in the surface reflectance ratios from low-flying aircraft data covering five months period over two years. The ratios showed angular variation with the values increasing in forward scattering direction. Further, the correlation also varied from very low during April and October to high during March and July. The points contributing to reducing the correlation in the April and October data were identified as due to observations been made in the forward scattering directions. Removing these points improved the correlation and also brought the slopes closer to the values given by Equation 2.3. Especially when the observations are made under conditions of specular reflection, the spectral dependence of the surface reflectance, responsible for the empirical relations in Equation 2.3, gets reduced. This is because under conditions of specular reflection, the incident light gets reflected from the surface of the plant itself. It doesn't interact with the canopy and hence the spectral signatures are missing. These results were corroborated by measurements during SCAR-B and other studies [Gatebe et al., 2001].

Besides the angular dependence inherent in the data, the overall dataset also showed the seasonal dependence of the surface reflectance ratios. Especially, with the advance of the growing season, the ratios decreased in value. A negative correlation was observed vis-a-vis the NDVI viz, during the months when NDVI had higher values, the ratios decreased from their predicted values. The seasonal variation in NDVI is expected since it is the difference between the surface reflectance at wavelengths where the surface is highly reflecting and that at which it is dark so that any changes in the surface reflectance due to the seasonal land changes will be reflected in the NDVI as well. But the empirical relations in Equation 2.3 are the ratios of surface

reflectance at two wavelengths at both of which the surface is dark so that such seasonal variation was not expected. Though the correlation between the surface reflectance ratios and NDVI of the surface is weak, still some features were observed. First, the ratios decrease with increase in NDVI. Secondly, the data points having the highest NDVI contribute maximum to the decrease in the value. These factors cue at the need for inclusion of NDVI parameterization in the empirical relations. In the updated version, the surface reflectance at red is parameterised in terms of the surface reflectance at 2130 nm and is a function of scattering angle, which is defined as:

$$\Theta = \cos^{-1}(-\cos\theta_0 cos\theta + \sin\theta_0 \sin\theta \cos\phi) \tag{2.4}$$

where θ, θ_0 and ϕ are the satellite zenith angle, solar zenith angle and the relative azimuth angle respectively, and the NDVI of the target

$$NDVI_{SWIR} = \frac{\rho^m_{1240} - \rho^m_{2120}}{\rho^m_{1240} + \rho^m_{2120}} \tag{2.5}$$

where ρ_{1240} and ρ_{2120} are the MODIS measured reflectances at the 1240 and 2120 nm wavelengths respectively. The surface reflectance value at blue wavelength is found from the value at red [Levy et al., 2007b].

The aerosol models in the version 4 algorithm were inferred based on the information regarding aerosol climatology available at that time. With the deployment of worldwide AERONET network, detailed information about the aerosol properties are available at more geographic locations [Holben et al., 1998]. The updated MODIS algorithm uses the aerosol models classified using all the AERONET data processed as of February 2005. The procedure includes the cluster analysis of the AOD data from AERONET divided into different optical depth bins and sorted according to their single scattering albedo. Such analysis classified the AERONET data into different aerosol models viz., spheroid and three fine aerosol models- absorbing (ω =0.85), moderately absorbing (ω =0.90) and non-absorbing (ω =0.95) aerosol types [Levy et al., 2007a].

Other special features of the updated MODIS aerosol product include the adjustment of the cloud mask, mass concentration, subpixel snow mask, improved estimation of the Rayleigh optical depth and approval of negative aerosol optical depths. In addition, the look-up table is examined through the AOD at 550nm as against the independent retrievals in 470 and 660 nm channels in the version 4 algorithm [Levy et al., 2007b], Remer et al. [2006].

At the operational stage, over dark surfaces, the C005 algorithm compares a weighted sum of fine dominated and coarse dominated aerosol models with the MODIS observed spectral reflectances. Simultaneous inversion in three channels viz., 470, 660 and 2130 nm is performed to retrieve values of τ_{550} (optical depth at 550 nm), η_{550} (weighting parameter, which represents the fraction of optical depth at 550 nm contributed by fine model aerosol) and ρ^s_{2120} (surface reflectance at 2120 nm). In addition, an alternative procedure similar to Remer et al. [2005] is followed for retrieval over brighter surfaces ($\rho^s > 0.25$) assuming continental aerosol model. The accuracy of this path is less than that for dark surfaces.

2.3 The Deep Blue Algorithm

Owing to the enormous importance of aerosol optical depth retrieval over land, especially over regions of higher surface reflectance, search is continuously made for alternative methods other than modifications to the existing algorithms as described in the previous section. It is in this light that the Deep Blue algorithm was proposed by Hsu et al. [2004] for SeaWiFS and MODIS-like sensors having wavelength channels in the blue region of the visible spectrum. This is of special interest since it is claimed to be highly efficient for aerosol retrieval over 'bright-reflecting' source regions like deserts, arid and semi-arid and urban areas. Currently it is not retrieving values over ice and snow areas. Initial retrieval exercises by Hsu et al. [2004] and Hsu et al. [2006] over Africa, ACE-Asia campaign and UAE have justified the claims and for this reason, the retrieved datasets from MODIS wavelengths have been included in the updated MODIS aerosol product as an alternative set. Currently, Deep Blue aerosol product from only Aqua platform is

available. Here we give a brief account of the Deep Blue algorithm details of which can be found in Hsu et al. [2004] and Hsu et al. [2006].

The underlying principle remains the same as in other retrieval algorithms. The radiance measured by the satellite sensor is composed of the contribution from the atmosphere, which includes the gas and aerosol scattering and absorption, and is known as the path radiance and the surface reflectance. Over land surfaces, the surface reflectance constitutes the biggest source of error on the retrieved aerosol parameters. For low reflectance surfaces, the retrieval can be made based on the empirical relations Equation 2.3 upto a considerable level of accuracy as described earlier. But for surfaces with extremely high reflectance like desert (40%), snow, arid etc, where the surface reflectance dominates over the path radiance, the retrieval becomes very difficult and error prone. This is because the observed radiance at the sensor height becomes fairly defined by the surface reflectance and less by the atmospheric contribution. For example, in the case of non-absorbing aerosols, the TOA reflectance becomes less and less dependent on the aerosol amount (AOD) with an increase in the value of surface reflectance. In the case of absorbing aerosols, the presence of aerosols increases the radiance over low reflecting surfaces and diminishes that over high reflecting surfaces. There exists, thus, a critical value of surface reflectance where the TOA radiance is not at all affected by the presence of aerosols. It yields, thus that in either case, the feasibility of aerosol retrieval over such regions is highly dependent on the absorption properties of the aerosol and the critical reflectance. The surface reflectance at red wavelength is extremely high over these regions so that the aerosol effects are not tangible. For higher values of aerosol optical depth this channel has been used with limited accuracy but for low aerosol loading, in which case the surface reflectance is considerably higher than the atmospheric path radiance, the retrieval would be treated as unsuccessful. But these surfaces are comparatively dark in the blue region of the visible spectrum so that in case retrieval is made using these channels, error in the results will be less. It has its own drawbacks though. The optical properties of dust aerosols is highly variable at blue wavelength than red and this effect will be more pronounced for higher aerosol loading. The Deep Blue

algorithm, which as its name suggests utilizes the radiances measured in the blue section of the spectrum, gets around this problem by using only blue channels (412 and 470 for MODIS and 412 and 490 for SeaWiFS) for low aerosol loading in order to avoid the high reflectance in red channel. For high aerosol loading, where the variability in the aerosol optical properties will affect the retrievals, red channel (660 nm) is also included to compensate the effect. The above procedure is followed for dust dominated areas. For regions having mixed aerosol type, the algorithm utilizes a linear combination of the dust and smoke aerosol contribution and derives the fraction of the dust dominated radiance.

For the operational process, at the pre-processing stage itself, gas absorption and cloud contamination is accounted for. Two approaches are used for the cloud rejection process. First is the usage of 412nm reflectance to identify the cloudy pixels owing to the higher reflectance of clouds at this wavelength. Next step consists of evaluation of the Deep Blue aerosol index which, taking advantage of the flat reflectance variation of clouds at 412 and 470nm as compared to the dust aerosols, offers a reliable way to identify clouds from heavy dust. After cloud screening, evaluation of the surface reflectance is the next important step.

The most crucial part of any algorithm meant for aerosol monitoring over land is the task concerning surface reflectance. The Deep Blue algorithm makes use of precalculated surface reflectance database using the minimum reflectivity technique. Using a vector radiative transfer code [Dave, 1970] to include polarization effects, lookup tables are created for satellite observed radiances. Then assuming a Rayleigh atmosphere and a Lambertian surface, Lambert equivalent reflectivities (LER) are computed on a 0.1 deg latitude $\times$ longitude scale. To circumvent the problem of cloud shadows, surface reflectivity corresponding to 412 nm channel is extracted because of the least error at this channel due to cloud shadows. The corresponding values for other wavelengths are then obtained. This approach of finding the reflectivity is same as the ones used by Herman and Celarier [1997] for TOMS data and Koelemeijer et al. [2003] for GOME data.

Having the values of all the necessary parameters and the look up table

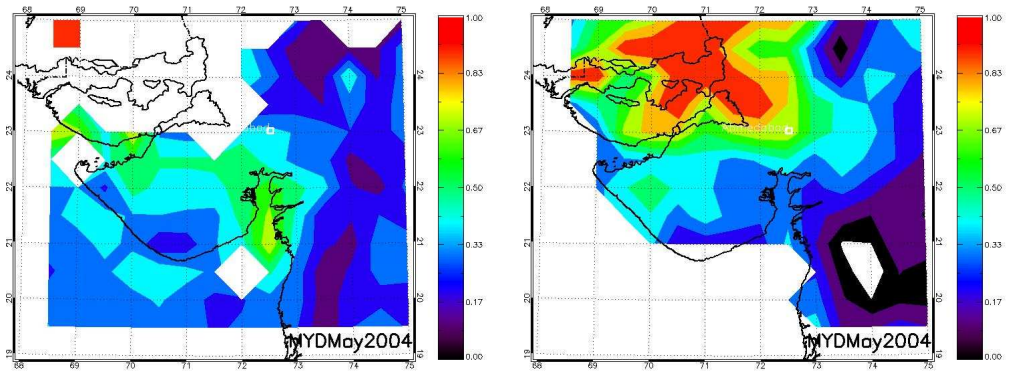

Figure 2.2: A comparison of MODIS retrieved AOD maps from Collection version C005 (left) and the Deep Blue algorithm (right). Data from the Aqua platform has been used. Deep Blue algorithm fills in various missing values in the C005 maps especially over the highly reflecting surfaces such as the Rann of Kuchh in North-West Gujarat. Presenly, Deep Blue algorithm is not providing retrievals over ice, snow and water bodies (Michael King, *personal communication*).

intact, the final step is the retrieval of the aerosol optical depth values. Here two different approaches are used for dust and mixed aerosol types. For dust dominated scenes, two different approaches are followed based on the amount of aerosol loading. This is because the contribution to TOA radiance which comes from surface reflectance is higher when aerosol loading is less. This is especially so at 660 nm and hence due to the corresponding errors being high, radiances at this channel cannot be used for retrieval. Thus, for low aerosol loading ($\tau < 0.7$), retrieval of aerosol optical depth and single scattering albedo is made at 412 and 470 nm wavelengths by matching the measured radiances with the simulated values using the maximum likelihood method. Even though the errors due to surface reflectance is less when 412 and 470 nm wavelengths are used, still the higher variability of aerosol optical properties at these two wavelengths as compared to at 660 nm is a limitation for this approach. The errors related to this effect will be more pronounced when aerosol loading is high. So, for higher aerosol optical depth ($\tau > 0.7$) values, 660 nm is also included in the retrieval scheme to assuage this effect. This technique is expected to retrieve aerosol optical depth values

when surface reflectance at 670 nm is upto 0.3. AOD retrieval over surfaces with reflectance as high as 0.4 at 670 nm can also be accomplished provided AOD is greater than 0.7. For retrieval of aerosol optical depth for mixed aerosol type, a mixture of dust and smoke aerosols are taken and retrieval is accomplished using the 412 and 490 nm channels. The maximum likelihood method is used with the lookup tables to derive the AOD which best fits the satellite measured radiances.

Figure 2.2 illustrates an application of this algorithm where AOD maps of Gujarat on 0.5 degree latitude $\times$ longitude grid is shown from MODIS C005 (left) and Deep Blue (right) aerosol products. The North-West region of the state, known as the Rann of Kuchh, is a vast deposit of highly reflecting salt. Aerosol remote sensing over this region is highly challenging because of the extremely high value of surface reflectance as can be seen in the map from C005 data product which reports missing values. However, the Deep Blue algorithm fills in the gaps in the conventional aerosol product. The missing values over Arabian sea in the Deep Blue product map is because this algorithm presently does not report results over liquid water and ice covers.

Based on the results of initial validation studies, Hsu et al. [2004] set the uncertainty level of the Deep Blue algorithm derived aerosol optical depth values at 20-30%. The main sources of error in the retrieval algorithm are surface reflectance, aerosol vertical profile and shape of the aerosol particles.

Chapter 3

Ahmedabad Meteorology

The present work concerns with a detailed study and validation of the MODIS aerosol product and investigate the spatial and temporal variations in the correlation coefficients of the validation results. Validation at different geographical locations provides insight into environments for which the retrievals are valid whereas validation carried out at a fixed location for an extended period of time provides details regarding the particular seasons and meteorological conditions when the retrieval is valid and identify the cases where further improvement can be made.

The location under study for temporal analysis of MODIS aerosol product is Ahmedabad (72.53^0 E, 23.03^0 N) in the western Indian state of Gujarat. The entire region is semi arid and is influenced by the Thar Desert in the North and Arabian Sea in the south-west. The local meteorology is summer from March to May, monsoon during June to September and winter from October to February.

In the present study, the annual dataset has been divided in four major seasons, viz, Dry(December to March), Pre-Monsoon(April and May), Monsoon(June to September) and Post-Monsoon(October and November) based on the variation of various meteorological parameters like wind speed and direction, temperature and relative humidity.

The relative humidity is usually less than 30% during Dry months and between 30-40% during Pre-Monsoon and Post-Monsoon months. Monsoon

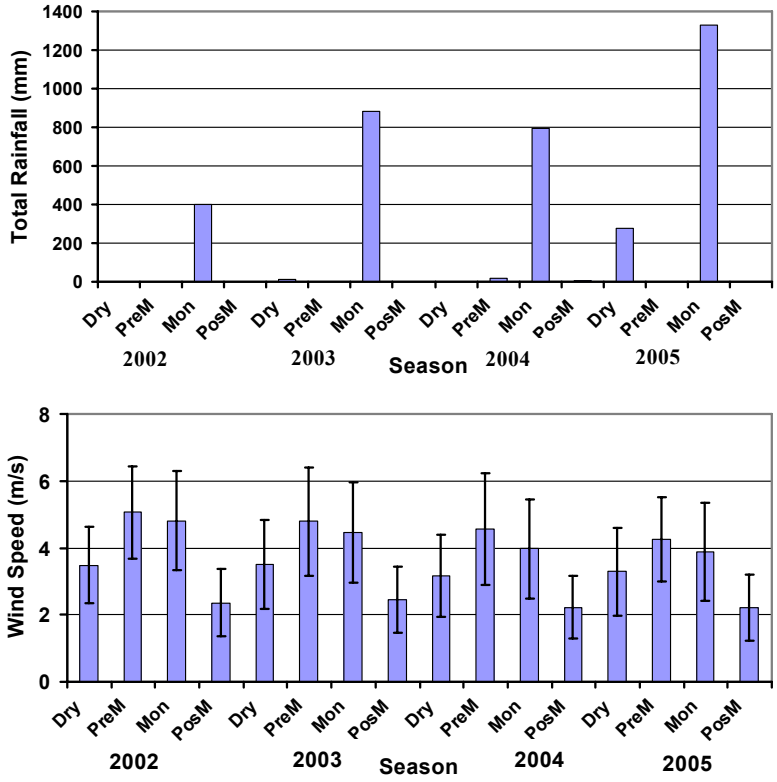

Figure 3.1: Variation of rainfall and wind speed during the study period, January 2002 to December 2005 over Ahmedabad, classified according to seasons, Dry(D, J, F, M), Pre-Monsoon(A, M), Monsoon(J, J, A, S) and Post-Monsoon(O, N)

season exhibits the highest value among all the seasons with RH crossing 70%. The average mean daily temperature during Dry season lies in the range of 22-24^0 C whereas during Pre-Monsoon season it is around 32^{0}C [Ganguly et al., 2006a].

Wind speed is highest(about 5 m/s) during Pre-Monsoon months closely followed by Monsoon months. It is lowest(about 2 m/s) during Post-Monsoon season and increases slightly during Dry season. Average value of wind speed showed a gradual decrease from 2002 to 2005. Amount of rainfall exhibited an increase during the study period. Thus the rainfall amount during 2002 was very less(400 mm). During 2003, Ahmedabad received comparatively more

rainfall but with large variabilities. During 2005, the rainfall amount was the highest (about 1300 mm) among all the years and it was also uniformly distributed throughout the season (Figure 3.1).

Figure 3.2 shows the overall pattern for aerosol optical depth distribution over Gujarat at 550 nm. It is derived by averaging the Level 2 aerosol data product from Aqua platform on a 0.5^0 latitude $\times$ 0.5^0 longitude scale. While finding the monthly average, a particular grid box was chosen only if daily averaged data for at least 10 days was available for that particular box. The images shown are for 2004 whereas the complete cycle of AOD variation can be seen at http://www.prl.res.in/∼amisra/gujarat.html. The regions of highest AOD (greater than 0.6) are located over North-West Gujarat and over the Gulf of Khambhat whereas the AOD over North-East and South-West regions are comparatively low(less than 0.15). The overall pattern of distribution is similar over the years but the actual magnitude of the AOD value is different. The higher value of aerosol optical depth over the NW Gujarat is mainly due to the area being less vegetated. This is the region of the Rann of Kuchh -a marshy deposit of salt. Aerosol remote sensing from satellite means is specially challenging over this region because of the surface being highly reflecting. The higher wind speeds over the region further aid in lifting the salt particles into vertical column, increasing the aerosol content.

AOD pattern vis-a-vis meteorology

Any study of the validation results has to be done taking into account the variation in the various meteorological parameters. Such a comparative study will aid not only in getting the overall view of the scenario during the study period but also in interpreting the various validation results in the light of various plausible causes. The main factors which govern the production and loss of the natural aerosol particles are wind, humidity and rainfall. For example, a higher wind speed aids in releasing more soil derived aerosol particles in the atmosphere resulting in an increased columnar aerosol content. Increase in relative humidity results in hygroscopic growth of smaller particles thus increasing the integrated aerosol optical depth. Due to rainfall, the

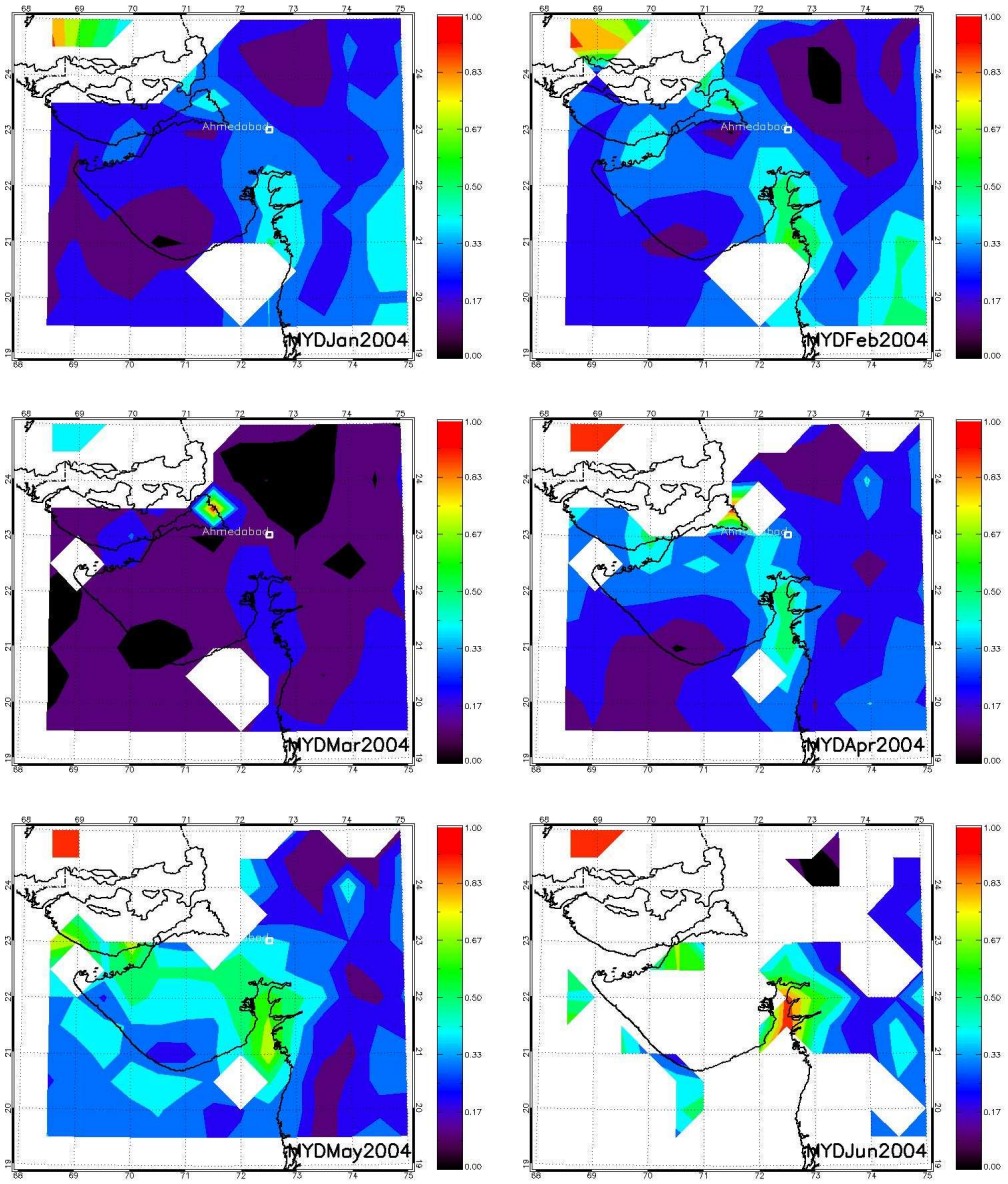

Figure 3.2: 0.5 degree averaged map of Aerosol Optical Depth at 550 nm over Gujarat during 2004. The complete dataset can be accessed at http://www.prl.res.in/∼amisra/gujarat.html

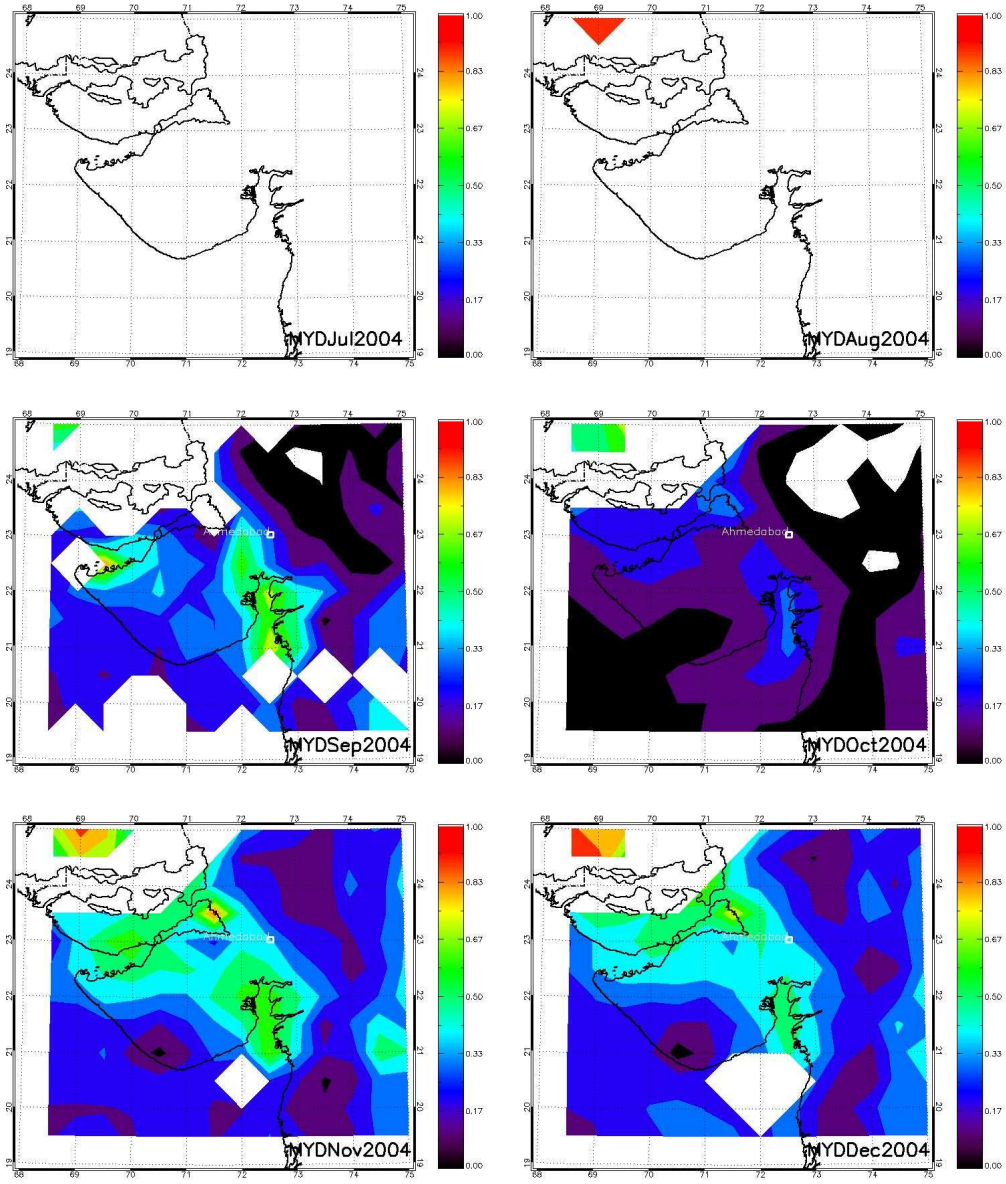

Figure 3.2: Contd.

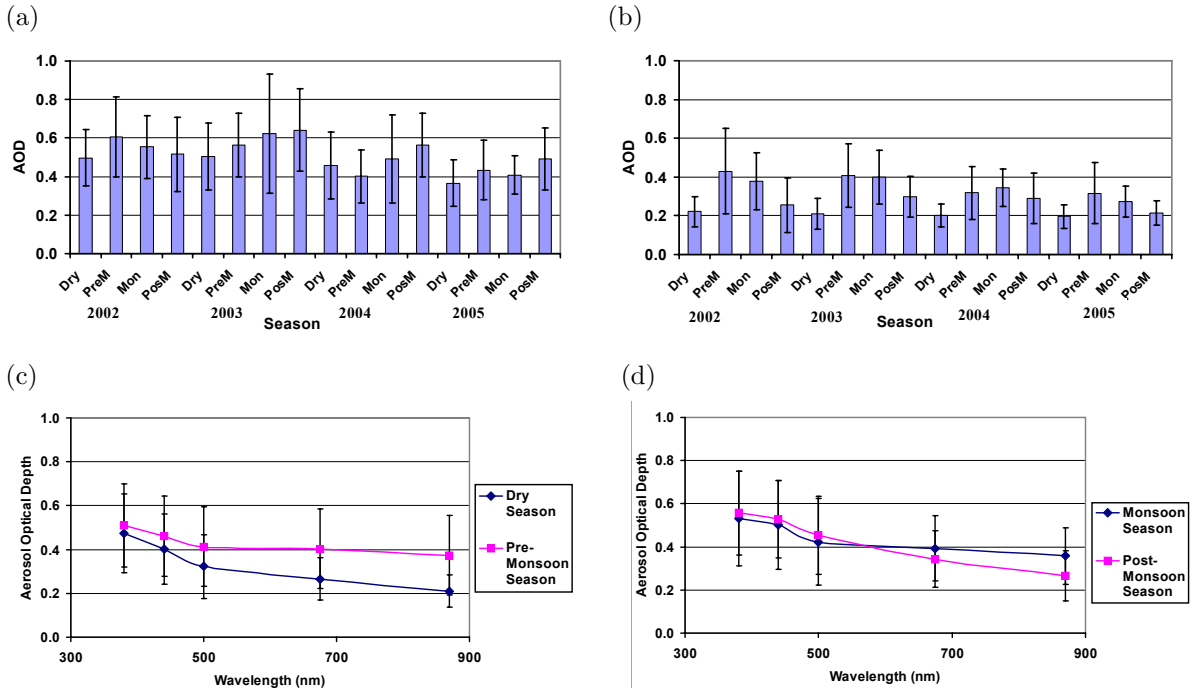

Figure 3.3: Observed variations in aerosol optical depth over Ahmedabad during the study period (2002-2005). (a) AOD at 380 nm (b) AOD at 870 nm (c) average AOD spectra for Dry and Pre-Monsoon seasons and (d) average AOD spectra for Monsoon and Post-Monsoon seasons (Ganguly et al. [2006a])

soil becomes damp restricting the possibility of soil derived particles being released. This, together with wet removal of aerosol particles leads to a reduction in AOD values. Dispersion of aerosol particles with wind is another loss process. The net amount of aerosol particles in the atmosphere depends on the dominant process and the size of the aerosol particles since different sized particles respond differently to the various meteorological changes. Thus, soil derived dust particles are generated with higher wind speed and are settled with rain. As compared to the natural aerosols which have a large seasonal variation, the smaller anthropogenic aerosols have less seasonal variation. A moderate value of wind speed is sufficient for dispersal of these particles to the neighbouring places.

The variation in the ground based sun-photometer measured columnar

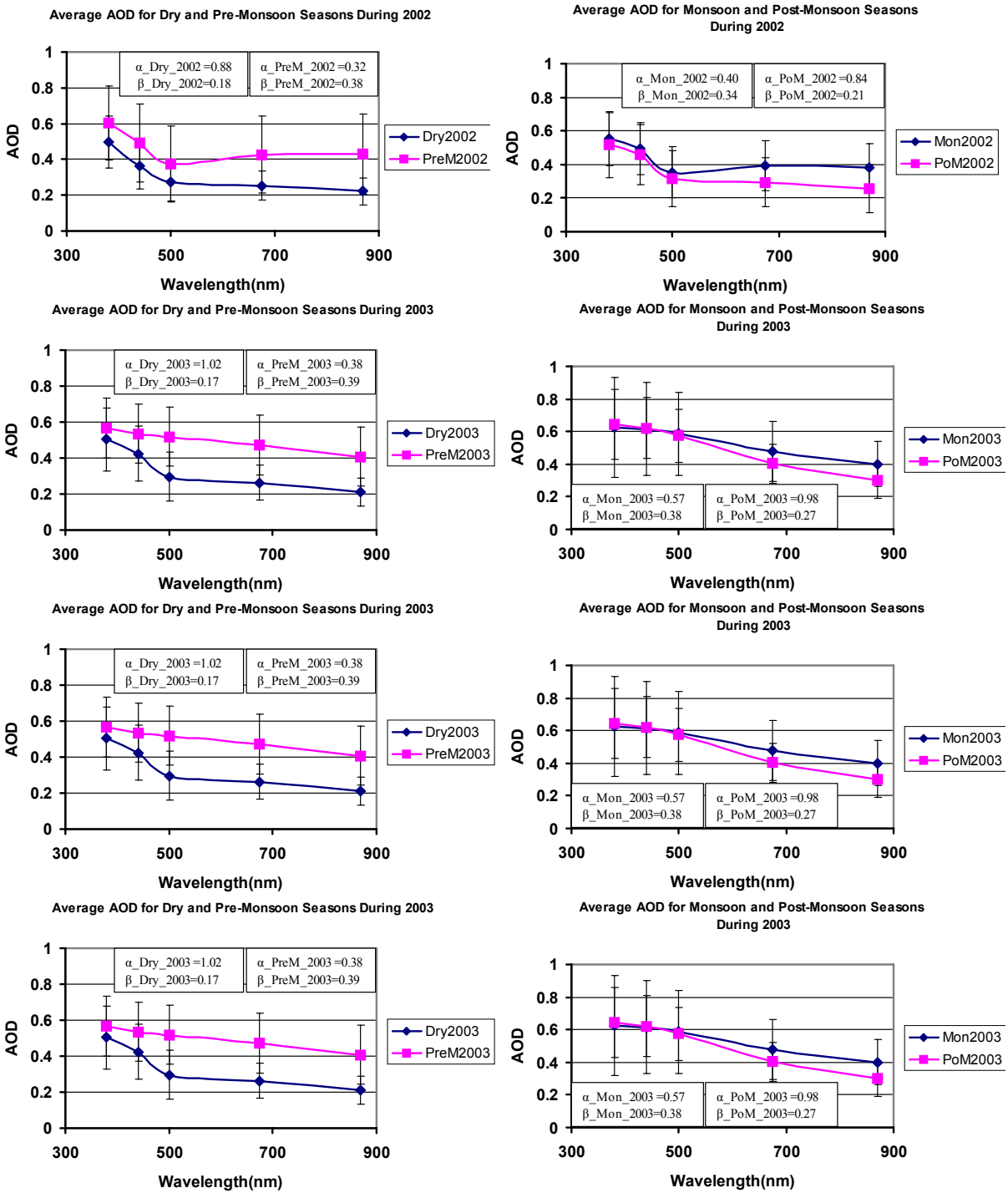

Figure 3.4: Observed average AOD spectra for different seasons for individual years during the study period (2002-2005) over Ahmedabad (Ganguly et al. [2006a]).

aerosol optical depth over Ahmedabad [Ganguly et al., 2006a] at two representative wavelengths, disaggregated into different seasons are shown in the Figure 3.3a and 3.3b. Also shown is the behaviour of the spectral aerosol optical depth for the different seasons (Figure 3.3c and 3.3d). These features can be grossly interpreted in terms of the meterological variables esp, the wind speed and rainfall amount. The aerosol amount during Dry season is in general low at all wavelengths. During Pre-Monsoon season, the wind speed increases leading to an increase in the AOD value which is more pronounced at higher wavelengths due to the production of soil derived dust particles. During Monsoon months, as the wind speed is similar to that during Pre-Monsoon months, there is no considerable change in AOD at higher wavelengths. But the AOD at lower wavelength show a marginal increase due to hygroscopic growth of particles as well as an increase in the boundary layer height which provides more accomodation space for the aerosols. The wind speed during Post-Monsoon season is the lowest and hence the production of soil derived dust particles becomes less. Also, the wet soil and increased vegetation after the monsoon reduce natural aerosol particles from being released from the surface. Thus the AOD at higher wavelengths is reduced due to a reduction in the dust derived aerosol component in the atmosphere. But the AOD at lower wavelengths maintains its value since the boundary layer height is still large. The boundary layer height decreases during the Dry season so that the AOD values at all the wavelengths are lowest during this season [Ganguly et al., 2006a].

Figure 3.4 shows the average AOD spectra for different seasons during individual years of the study period. It is seen that the variation with season at smaller wavelengths is mostly within the standard deviation, whereas that at higher wavelengths is large. This means that the smaller particles, which are mostly anthropogenic in nature, are not affected by natural processes. However, the AOD at higher wavelengths has large variation with season since they are naturally derived particles and are more affected by natural processes. This is the trend in AOD as observed from ground based measurements and is considered to be correct since it is free from the usual errors affecting the satellite based measurements. Since recent studies have shown

the capability of MODIS to provide information about fine particle content in the atmosphere [Kaufman et al., 2005], it is interesting to see whether such seasonal and annual variations are reflected in the satellite dataset as well.

Chapter 4

Instruments

Satellite and ground based measurements follow different methods to derive the aerosol content in the atmosphere, each having its advantages and limitations. Ground based sunphotometer measurements are more accurate being based on direct observation of solar radiation and do not require information about aerosol type. But they are point observations and cannot provide details of spatial variation of aerosols. Satellite measurements, on the other hand, offer long-term routine unmonitored remote sensing of aerosols with a wide spatial coverage, but are hindered by errors due to surface reflectance, aerosol type related uncertainties and cloud contamination. Since each method follows different procedure to retrieve the aerosol properties, it is necessary to have information regarding the instrument whose data is to be validated and the instrument providing the validating dataset. Here we first discuss the details of the MODIS instrument, its technical specifications and the various levels of data products. Next, the Microtops sunphotometer and its basic principle of working are outlined. Finally, we provide the details of data analysis followed to process the two sets of data for the validation exercise, results of which are discussed at length in the next two chapters.

4.1 MODIS

The Moderate Resolution Imaging Spectroradiometer (MODIS) is an EOS facility instrument, launched aboard NASA satellites Terra and Aqua in December 1999 and May 2002 in sun-synchronous orbits with equator crossing times of 10:30 a.m and 1:30 p.m. respectively. Its $\pm 55^0$ scanning pattern at an orbit of 705 Km results in a large swath of 2330 Km and provides global coverage every 1-2 days. With a sophisticated onboard calibration, observations are made in a large spectral span of 36 channels from 0.4 μm to 14 μm at spatial resolutions of 250 m (bands 1 and 2), 500 m (bands 3 to 7) and 1 km (bands 8 to 36).

A special feature of MODIS is the availability of 17 bands for detecting clouds, shadows, fires and heavy aerosol loading alongwith the ability to detect cirrus clouds and resolve boundary layer cloud fields [King et al., 1999]. Further, having the instrument with nearly same technical specifications on two platforms, providing similar products, makes the study of diurnal variation of atmospheric properties feasible. The MODIS radiance data is inverted into nearly 40 different products having applications in various fields of considerable interest and importance in the Earth system studies such as land, atmosphere and ocean processes. Surface temperature, ocean colour, chlorophyll fluoroscence and concentrations, vegetation and land-surface cover, snow and sea ice cover, land-surface reflectance, cloud cover, cloud and aerosol properties, fire occurance, precipitable water and cirrus-cloud cover are some of the data products available from MODIS [EOS Data Products Handbook, Vol 2, 2000].

Table 4.1 gives the technical specifications of the MODIS instrument and an overview of the various atmospheric data products available is shown in Figure 4.1.

4.1.1 MODIS Instrumentation

Selection of the 36 bands for MODIS derives from the experience gained from previous sensors. Thus, the bands 1-7 used for the land cover, cloud and aerosol studies are similar to those of Landsat TM, ocean colour bands

8-16 are derived from Coastal Zone Colour Scanner(CZCS) and SeaWIFS, bands 20-25 are from High Resolution IR Sounder(HIRS) for troposphere and surface properties related studies.

The basic measurement principle of MODIS is as follows. A double-sided beryllium scan mirror reflects the energy from its earth view, which is received by an afocal Gregorian telescope. This energy, in turn, is transmitted to the Focal Plane Assemblies after passing through beam splitters and refractive objectives. Focal Plane Assembly output is the raw instrument data which is transmitted to the ground receiving station.

MODIS Focal Plane Assemblies include different detectors depending on the wavelength range. For visible and NIR (0.4μm to 1.0μm) p-i-n photovoltaic silicon diode; for SWIR, MWIR and LWIR (1.2μm to 4.5μm and <=10μm) photovoltaic HgCdTe detector; and for LWIR (>10μm) photoconductive HgCdTe is used. The instrument has four onboard calibrators- a Solar Diffuser, a Blackbody, a Spectroradiometric Calibration Assembly and a Solar Diffuser Stability Monitor [Barnes et al., 1998].

Orbit	705 km, 10:30 a.m. descending node or 1:30 p.m., ascending node, sun-synchronous, near-polar, circular
Scan Rate	20.3 rpm, cross track
Swath Dimensions	2330 km (across track) by 10 km (along track at nadir)
Telescope	17.78 cm diam. off-axis, afocal (collimated), with intermediate field stop
Size	1.0 × 1.6 × 1.0 m
Weight	250 kg
Power	225 W (orbital average)
Data Rate	11 Mbps (peak daytime)
Quantization	12 bits
Spatial Resolution	250 m (bands 1-2)
(at nadir)	500 m (bands 3-7), 1000 m (bands 8-36)
Design Life	5 years

Table 4.1: Technical Specifications of the Moderate Resolution Imaging Spectroradiometer

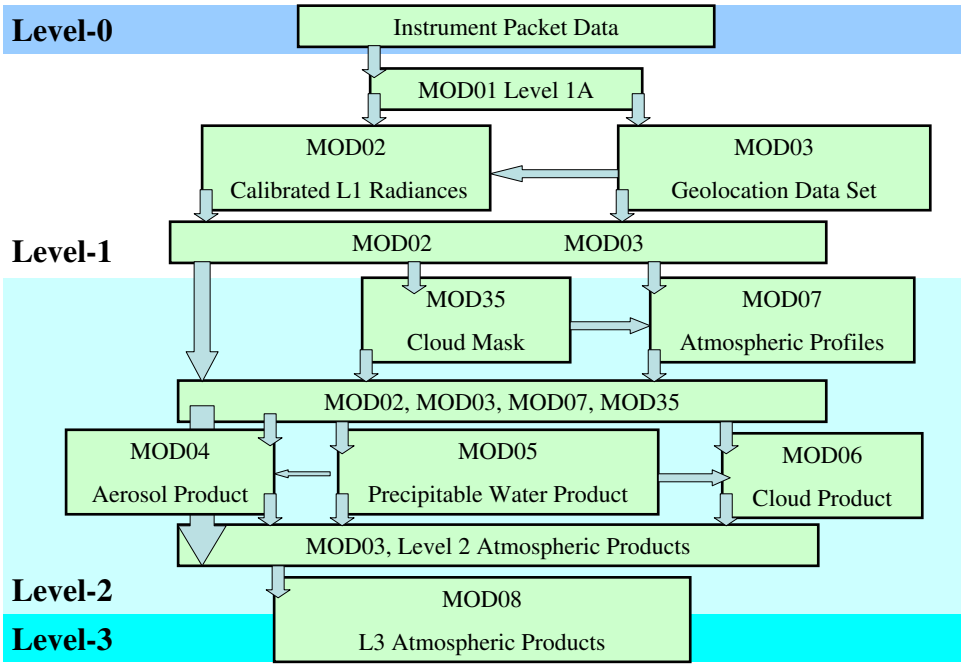

Figure 4.1: Various levels of atmospheric data products from MODIS [King et al., 2003]

4.1.2 MODIS Data Products

MODIS Sensor raw data in binary format is separated into 5-minute granules known as the **Level 1A** data and contains sensor's response, engineering and telemetry information.

This Level 1A data is processed using the geolocation and calibration information to arrive at the **Level 1B** stage. The procedure converts the Level 1A data into radiometrically calibrated and geolocated data. The output data product includes top of atmosphere reflectance factors for the Reflective Solar Bands (Bands 1-19 and 26), radiances for both the Reflective Solar Bands and Thermal Emissive Bands (Bands 20-25 and 27-31) and associated uncertainty indices and data quality flags. The data files also contain the geolocation information. Calibration of thermal emissive bands is performed using the on-board calibrator Black Body whereas that of the reflective solar bands is done by a Solar Diffuser panel. Depending on the spatial resolution, the Terra (Aqua) Level 1B data files are desig-

nated as MOD(MYD)02QKM (250 m) MOD(MYD)02HKM (500 m) and MOD(MYD)021KM (1 Km) [Xiong et al, 2006].

The Level 1B data is processed according to different algorithms corresponding to the particular parameter to be retrieved to arrive at the various categories of **Level 2** land, ocean, cloud, atmospheric profile etc data products. The present work utilizes the Level 2 aerosol product released by the MODIS atmosperic science team. Two different algorithms are used for aerosol retrieval over land [Kaufman et al., 1997a, Remer et al., 2005, Levy et al., 2007b] and ocean [Remer et al., 2005, Tanré et al., 1997] because of the different environmental conditions. Higher value of surface reflectance in addition to surface heterogeneity and variability of surface characteristics makes aerosol retrieval over land difficult. Essential elements of aerosol retrieval algorithm over land have already been mentioned in Chapter 2. Several datasets of interest to Earth and atmospheric science community form part of the Level 2 aerosol product some of which (from retrieval over land) are listed in Table 4.2. Each dataset corresponds to a 5-min granule of the MODIS path with spatial resolution of $10km \times 10km$. In addition, solar and satellite geometry, and geographical information is also included. The Level 2 aerosol product filenames are designated as MOD(MYD)04_L2 for datafiles from Terra(Aqua) MODIS [Remer et al., 2005].

Level 2 aerosol, cloud, precipitable water and atmospheric profile data products are combined to arrive at the joint **Level 3** atmospheric data product. This data product is provided on a $1^0 \times 1^0$ equal angle global grid. In addition, statistics derived from the Level 2 products such as mean, standard deviation, parameters of normal and log-normal distributions, fractions of pixels satisfying particular condition etc. are also included. Level 3 data is produced for three time intervals and accordingly their nomenclature is different: MOD(MYD)08_D3 (for daily), MOD(MYD)08_E3 (for eight days average) and MOD(MYD)08_M3 (for monthly average) for the Terra (Aqua) platform [King et al., 2003].

Corrected Optical Depth	STD Reflectance Reflectance
Optical Depth Ratio Small	Quality Assurance
Mass Concentration	Path Radiance
Angstrom Exponent	Error Path Radiance
Reflected Flux	Critical Reflectance
Transmitted Flux	Error Critical Reflectance
Aerosol Type	Quality Weight Path Radiance
Continental Optical Depth	Quality Weight Critical Reflectance
Estimated Uncertainty	Quality Assurance Critical Reflectance
Mean Reflectance All	Deep Blue Aerosol Optical Depth 550
Standad Deviation Reflectance All	Deep Blue Aerosol Optical Depth
Cloud Fraction	Deep Blue Angstrom Exponent
Number of Pixels Percentile	Deep Blue Single Scattering Albedo
Mean Reflectance	Deep Blue Surface Reflectance

Table 4.2: Main datasets which are part of the MODIS Level 2 aerosol product. Only the datasets over land are mentioned. Presently, Deep Blue Algorithm data is available only from Aqua MODIS.

4.2 Microtops sunphotometer

The Microtops sunphotometer provides the ground truth data for the validation [Morys et al., 2001]. Regular observations of columnar aerosol optical depth with the instrument are being carried out since 2002. The instrument provides the measurement of aerosol optical depth at 380, 440, 500, 675 and 870 nm wavelengths with uncertainty less than 0.03. A second Microtops sunphotometer is used to derive AOD at 1020 nm and total columnar ozone and water vapour concentrations. The derivation of aerosol optical depth is based on the attenuation of direct solar radiation by the atmospheric column and requires correction for gaseous absorption and Rayleigh scattering. The underlying principle is the Beer- Bouguer- Lambert law [Liou, 2002]

$$I(\lambda) = \left(\frac{r_0}{r}\right)^2 I_0(\lambda) exp[-\tau(\lambda) m(\theta_0)] \tag{4.1}$$

Here, r and r_0 are the actual and mean sun-earth distances, θ_0 is the solar zenith angle, $\tau(\lambda)$ is the optical depth and $m(\theta_0) = 1/cos(\theta_0)$ is the air mass

factor defined as the ratio of the actual and vertical path lengths of the radiation through the atmosphere to the instrument [Morys et al., 2001]. It is derived using the empirical relation given by Young [1980]

$$m(\theta_0) = \frac{1.002432\cos^2(\theta_0) + 0.148386\cos(\theta_0) + 0.0096467}{\cos^3(\theta_0) + 0.149864\cos^2(\theta_0) + 0.0102963\cos(\theta_0) + 0.000303978} \tag{4.2}$$

$I(\lambda)$ denotes the solar intensity measured by the ground based instrument whereas, $I_0(\lambda)$ is the solar intensity at the top of the atmosphere. The optical depth $\tau(\lambda)$ is obtained by taking logarithm of Equation 4.1

$$\tau_\lambda = \frac{-1}{m}\left[\ln\left(\frac{I_\lambda}{I_{0\lambda}}\right) - 2\ln\left(\frac{r_0}{r}\right)\right] \tag{4.3}$$

The plot of $\ln I(\lambda)$ with m is a straight line which on linear extrapolation to $m = 0$ gives $I_0(\lambda)$. This method of evaluation of the solar intensity at the top of the atmosphere is known as the *Langley plot analysis*. A constant atmosphere, viz., absence of clouds and a stable aerosol layer, is necessary for a satisfactory Langley plot analysis. Aerosols generally reside at lower altitudes so Langley analysis is carried out at high altitude locations.

Regular calibration of Microtops sunphotometer is done on a regular basis at Mt. Abu. Comparison of Microtops sunphotometer with other sunphotometers has been done during ISRO GBP land campaigns 1 and 2 at Shadnagar (Hyderabad) and Delhi respectively.

During the inter-comparison of sunphotometers during ISRO-GBP Land Campaign-1, the mean of AODs measured by the institutes was found and scaling factor for each institute was derived. A scaling factor of 1 means that the mean AOD of that particular institute is the same as the all-institute 3-day mean, $scaling\ factor > 1$ meant overestimation and $scaling\ factor < 1$ meant underestimation. The scaling factor for PRL sunphotometer was 1.067 at 500 nm. The mean AODs at 500 nm were found to be in the range of 0.35 to 0.5.

From the inter-comparison exercise of Microtops sunphotometers from different institutes during ISRO-GBP Land-Campaign-2, it was found that the AOD measurements were consistent among themselves and were inconsistent only within ± 0.05. The mean AODs at 500 nm were found to be in the range 0.45 to 1.3. During winter season, the aerosol optical depths over the Indo-Gangetic plains are generally higher than the peninsular India so that uncertainties in the aerosol optical depth are less [Ganguly et al., 2006b]. It was concluded that no calibration or correction factors were needed for any of the sunphotometers.

4.3 Data Analysis

The MODIS level 2 aerosol data product from both Terra and Aqua platform is used in the present work. The data from the collection version 4 [Remer et al., 2005], the updated version 5 [Remer et al., 2006, Levy et al., 2007b] and Deep Blue algorithm [Hsu et al., 2004, 2006] are used.

For the present study, sunphotometer observations have been selected on the condition that the time difference between ground based observation and MODIS overpass time is less than or equal to half an hour. The MODIS derived AOD was averaged over 0.5^0 latitude $\times$ 0.5^0 longitude box centered over Ahmedabad. This is required to have a reasonable comparison between satellite derived values which are a spatially spread data with sunphotometer values which are point measurements. A larger box used for averaging will introduce aerosol type and topography related uncertainties whereas any smaller box will include very few data points used for the averaging [Ichoku et al., 2002].

As MODIS provides AOD at 470 and 660 nm, none of which is present in the Microtops spectrum, the ground truth AODs at these wavelengths are found from the Angstrom Law fit [$AOD_\lambda = \mathrm{a}\lambda^{-b}$] of the sunphotometer wavelengths. Angstrom exponent computed from the AOD spectrum depends on the wavelength range chosen for computation. In general, in the presence of fine particles, Angstrom exponent computed from lower wavelengths is smaller than the one computed from the whole spectrum and also has a bet-

ter correlation with the particle size which reduces when longer wavelengths are used. Thus, Angstrom exponent computed from smaller wavelengths results in less uncertainty in the computed AOD at 470 nm which itself is affected by the fraction of smaller particles in the atmosphere. Similarly, the value of Angstrom exponent computed from higher wavelength is better correlated with particle size in the presence of coarse particles and results in lesser uncertainty in the computed AOD at 660 nm which is affected by the coarse particles in the atmosphere. This becomes specially important for particular seasons when the aerosol climatology is dominated by particles of a particular size, viz., fine particles during Dry and Post-Monsoon and coarse particles during Monsoon and Pre-Monsoon. Therefore in our study, AOD at 470 nm is evaluated using Angstrom exponent computed from AODs at 380-500 nm wavelengths whereas AOD at 660 nm was evaluated using Angstrom exponent computed from AODs at 500-870 nm. Apart from a combined comparison for the four years, the Ahmedabad data has also been separated between individual years and also grouped into different seasons as per the criterion described in the previous chapter. The next two chapters provide a detailed discussion of the validation exercise of the MODIS aerosol products under different geographical and environmental conditions.

Chapter 5

Validation Results for Ahmedabad

Before examining in detail the validation results over Ahmedabad, it is worth mentioning the results obtained by [Levy et al., 2005] during the CLAMS experiment since the results obtained there provided the impetus for the latest update to the MODIS aerosol product. According to [Levy et al., 2005], the offset in the correlation plot over land was more at blue than at red, while the slope was closer to unity at blue as compared to red and the correlation coefficient was also better at this wavelength. Further details in this regard alongwith the results from other validation groups are discussed in the concluding chapter.

5.1 Validation results of the C004 Aerosol product

5.1.1 Aqua

The time series of percentage difference in the MODIS retrieved and sunphotometer derived AOD is depicted in Figure 5.1, where,

$$\% \text{ difference} = \frac{\text{AOD}_{\text{MODIS}} - \text{AOD}_{\text{Sunphotometer}}}{\text{AOD}_{\text{Sunphotometer}}} \times 100 \qquad (5.1)$$

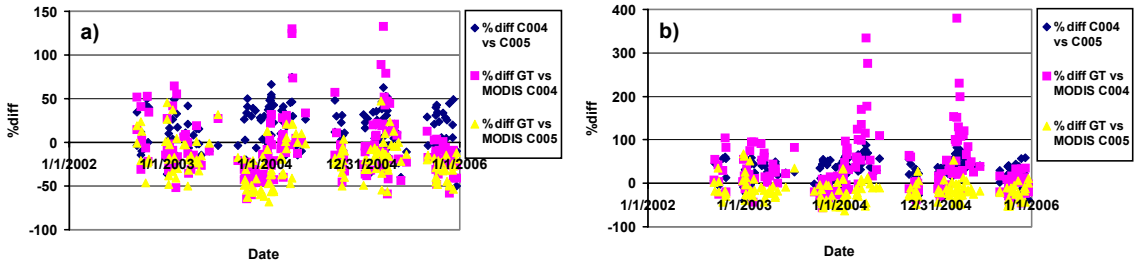

Figure 5.1: Time series of % difference (a) for 470 nm, (b) for 660 nm between different sets of data from both versions of MODIS algorithm and the Microtops Sunphotometer

The MODIS data in Figure 5.1 corresponds to two consecutive versions of the operational algorithm: the Collection Versions C004 and C005 from the Aqua platform. A positive value of the percentage difference implies an overestimation by MODIS. It is observed that the magnitude of the percentage difference is minimum during post monsoon months which increases as summer approaches. During May/ June owing to increased surface reflectance, the related errors increase. This feature is more pronounced during 2004 and 2005.

Figure 5.2 depict the comparison of C004 MODIS aerosol optical depth with the Microtops sunphotometer data for the period 2002 to 2005 [Misra et al., 2008]. Figure 5.2a is for 470 nm, 5.2b for 550 nm, while 5.2c is for 660 nm. The deviation from unity of the slope of correlation plot represents systematic biases and are mainly due to aerosol model assumptions, instrument calibration or the choice of the lowest 20-50 percentile of the measurements [Chu et al., 2002, 2003, Remer et al., 2005] whereas the intercept represents the errors due to surface reflectance assumptions. The large scatter seen in the plot is due to the comparison for 4 years of data which includes all seasons. Possibility of the comparison being better for some seasons than others can lead to large scatter. One of the ways in which it can affect the retrieval process is through the varying surface reflectance. It is seen that the spread in data is larger at red ($R^2_{660} = 0.25$) or in other words, correlation is better for blue ($R^2_{470} = 0.40$). Intercepts are nearly same in both cases (0.15 at blue

and 0.18 at red) but slope is closer to unity for red (0.65) as compared to blue (0.51). This is in marked contrast to the result inferred by [Levy et al., 2005] who found slope to be better at blue. The correlation coefficient results are consistent, however.

But the comparative results at the two wavelengths (such as here or in [Levy et al., 2005] should be treated with caution and not generalized to all cases. This is clear from our other plots over Ahmedabad (results given in tabular form in Table 5.1 where the combined data of Figure 5.2 has been disaggregated into separate years as well as different seasons as per the criteria discussed earlier. It is seen that the correlation of the two sets of data shows different behaviour at these two wavelengths depending on the season.

Comparison for different years

Year 2002 has the least amount of data since MODIS onboard Aqua was launched during May this year which was immediately followed by the Monsoon months leading to a scarcity of data during this period. Still, some features observed during this dataset show the correlation coefficient as well as intercept for C004 AOD data to be nearly same at both red($Intercept_{660} = 0.24$, $R^2_{660} = 0.21$) and blue($Intercept_{470} = 0.22$, $R^2_{470} = 0.23$) as shown in Table 5.1. But this time it is the slope at blue which has a better value($Slope_{470} = 0.46$, $Slope_{660} = 0.39$).

The above case reverses in 2003 where the slopes for C004 data have higher value at red(0.86) as compared to at blue(0.53). Correlation coefficients are nearly same for both the wavelengths ($R^2_{470} = 0.45$, $R^2_{660} = 0.46$) but intercept is larger for blue(0.12) than red(0.08).

The pattern of correlation for C004 reverses again for the year 2004 when the slope is larger and intercept lower at blue wavelength ($Slope_{470} = 0.52$, $Intercept_{470} = 0.17$) as compared to red ($Slope_{660} = 0.45$, $Intercept_{660} = 0.29$). Correlation coefficient is considerably higher at blue (R^2_{470} =0.34, R^2_{660}=0.14).

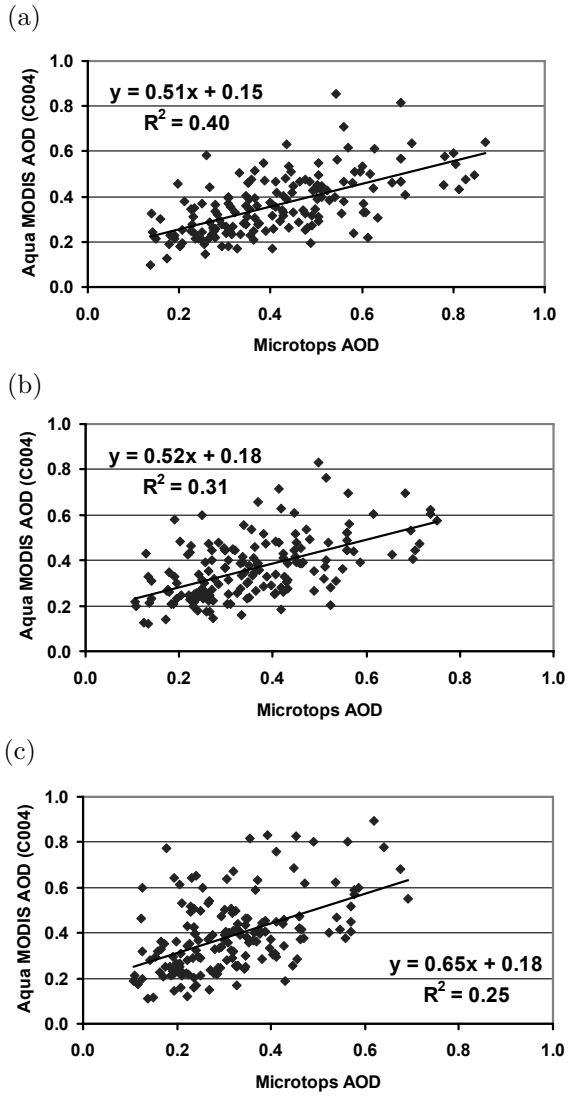

Figure 5.2: Validation Results of the MODIS aerosol product from Collection Version C004 from the Aqua platform at (a) 470nm (b) 550nm (c) 660nm

The slope pattern for C004 changes again during 2005 when the slope at red is larger than at blue whereas correlation coefficient is still quite larger at blue. Intercept at red is only marginally higher than at blue.

Comparison for different seasons

The comparison between MODIS and Microtops data has been disaggregated among different seasons according to the criteria described earlier.

During Dry season, for the C004 dataset, the correlation is much better at blue (R^2_{470}=0.47) than at red (R^2_{660}=0.19), while the slope as well as intercept are lower at blue.

In the Pre-Monsoon C004 dataset also, the correlation is very poor at red (R^2_{660}=0.18) as against that at blue (R^2_{470}=0.33). But this time slope at blue is closer to unity than at red. The intercepts are large at both wavelengths- being much higher at red (0.38) than at blue (0.18).

	470 nm			550 nm			660 nm		
Case	Slope	Intercept	R^2	Slope	Intercept	R^2	Slope	Intercept	R^2
Overall	0.51	0.15	0.40	0.52	0.18	0.31	0.65	0.18	0.25
2002	0.46	0.22	0.23	0.44	0.22	0.31	0.39	0.24	0.21
2003	0.53	0.12	0.45	0.55	0.14	0.41	0.86	0.08	0.46
2004	0.52	0.17	0.34	0.48	0.22	0.24	0.45	0.29	0.14
2005	0.57	0.12	0.40	0.64	0.14	0.29	0.82	0.14	0.22
Dry	0.51	0.14	0.47	0.54	0.16	0.33	0.65	0.18	0.19
Pre-Mon	0.55	0.18	0.33	0.46	0.29	0.21	0.46	0.38	0.18
Monsoon	0.84	0.10	0.45	0.97	0.07	0.49	1.10	0.06	0.43
Post-Mon	0.44	0.15	0.46	0.51	0.13	0.48	0.63	0.11	0.49

Table 5.1: Correlation Coefficients of Validation results of Aqua C004 aerosol product

Monsoon season suffers from the lowest number of data points used in the comparison because of generally overcast conditions during most of the days during this season. For the C004 version, slopes are quite large and much closer to unity (0.84 at blue and 1.1 at red) and intercepts are also lower (0.1 at blue and 0.06 at red) as compared to Dry and Pre-Monsoon months. The correlation coefficient is almost similar at both the wavelengths (0.45 at blue and 0.43 at red).

With the C004 version for the Post Monsoon months also, the correlation ($R^2_{470} = 0.46$ and $R^2_{660} = 0.49$) is nearly similar to that for Monsoon months and much better than for Dry and Pre-Monsoon season. Slope is not satisfactory (0.44 at blue and 0.63 at red) and intercept is also large(0.15 at blue and 0.11 at red).

Overall, a few points can be noted from the validation results of the Aqua MODIS C004 aerosol product. Correlation coefficients are better at blue than red for all years except for 2003 when they have nearly similar values. Intercepts are larger at red for all years except 2003 in which case intercept at blue is larger. Slopes of the correlation plot in this version do not show any particular pattern since for 2002 and 2004 slope at blue is more close to unity whereas for 2003 and 2005 as well as in the combined dataset, it is the slope at red which is larger [Misra et al., 2008].

5.1.2 Terra

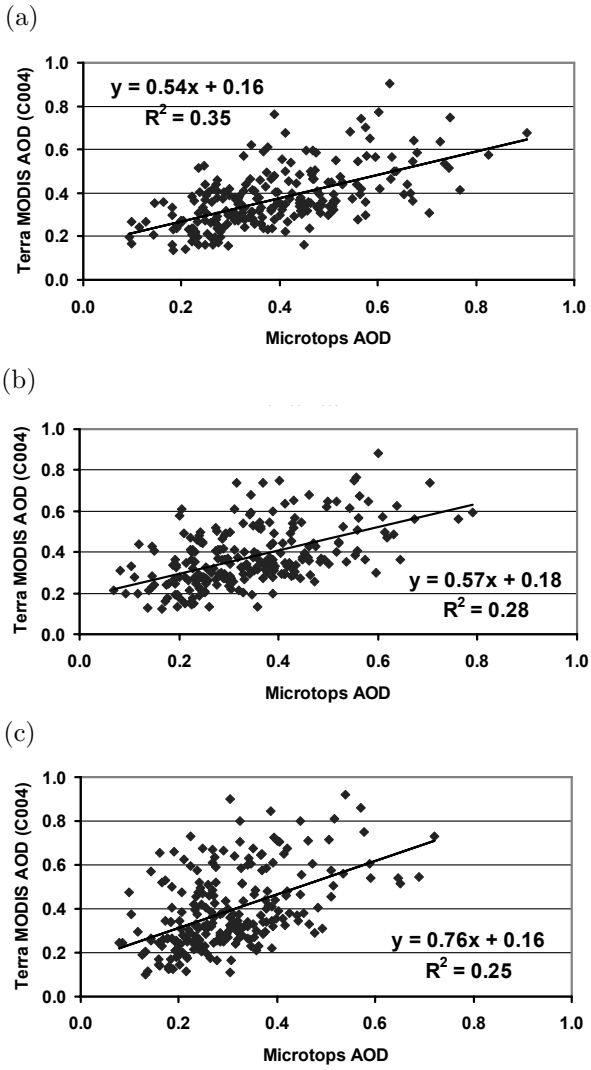

Figure 5.3: Validation Results of the MODIS aerosol product from Collection Version C004 from the Terra platform at (a)470nm (b)550nm (c)660nm

The validation of the Terra MODIS aerosol product is comparatively better because of larger dataset being available from this platform. Since Terra was launched in December 1999 and data from MODIS onboard this satellite is available from February 2000, the data corresponding to early 7 months of 2002, which were absent in Aqua dataset, are present in Terra data. Further, since the overpass time of Terra is during morning as against Aqua which has afternoon overpass, validation results may be affected due to changes in surface reflectance from morning to afternoon hours.

The validation results of MODIS C004 data product from Terra platform is shown in Figure 5.3. Here also we find the scatter in the data to be large at all wavelengths. In this data set as well, slope at red ($Slope_{660} = 0.76$) is found to be closer to unity than that at blue ($Slope_{470} = 0.54$). Similar feature was seen in the Aqua dataset

as well. Intercepts are exactly equal at both wavelengths ($Intercept_{470} = Intercept_{660} = 0.16$). But overall correlation is much better at blue ($R^2_{470} = 0.35$) than at red ($R^2_{660} = 0.25$), though lower than that for Aqua dataset. As in the previous case, the overall comparison has been disaggregated into different seasons and years to investigate any possible pattern in the correlation parameters.

Comparison for different years

Since Terra was launched in Dec 1999 and data from MODIS is available since February 2000, year 2002 which suffered from less amount of data in the Aqua study, has sufficient data points in the Terra dataset. Here we see the correlation to be slightly better at red ($R^2_{660} = 0.29$) than blue ($R^2_{470} = 0.26$). Slope at red is much closer to unity ($Slope_{660} = 0.78$) than blue ($Slope_{470} = 0.52$) whereas intercepts are also larger at blue ($Intercept_{470} = 0.20$, $Intercept_{660} = 0.17$).

For 2003, slope is better at red ($Slope_{660} = 0.78$) than blue ($Slope_{470} = 0.54$) and intercept is higher at blue ($Intercept_{470} = 0.17$) than at red ($Intercept_{660} = 0.12$). This is similar to the result obtained from the Aqua platform. But this time the correlation at red ($R^2_{660} = 0.29$) is much less than that noted in the Aqua case. Correlation coefficient at blue is $R^2_{470} = 0.40$.

Similar to the Aqua dataset during 2004, intercept at red ($Intercept_{660} = 0.22$) is higher than at blue ($Intercept_{470} = 0.16$) in Terra data as well. Similarly, correlation is much better at blue ($R^2_{470} = 0.35$) than at red ($R^2_{660} = 0.21$), but slope at red ($Slope_{660} = 0.63$) is better than that at blue ($Slope_{470} = 0.57$).

Interestingly, values of all parameters at blue ($Slope_{470} = 0.57$, $Intercept_{470} = 0.12$, $R^2_{470} = 0.39$) during 2005 are similar to those from Aqua platform. Further, the large scatter ($R^2_{660} = 0.26$) but higher value of slope at red ($Slope_{660} = 1.04$) is a feature similar to that from Aqua platform. But intercept at red ($Intercept_{660} = 0.07$) is lower than blue.

Comparison for different seasons

During Dry season, the pattern of correlation at blue and red is similar to that observed in Aqua MODIS. Thus correlation coefficient is much lower at red ($R^2_{660} = 0.10$) than at blue ($R^2_{470} = 0.32$). Similarly, slope as well as intercept is higher at red ($Slope_{660} = 0.47$, $Intercept_{660} = 0.19$) than at blue ($Slope_{470} = 0.39$, $Intercept_{470} = 0.17$).

During Pre Monsoon season, the comparison is better for Terra dataset ($R^2_{470} = 0.46$, $R^2_{660} = 0.40$). Intercept at red ($Intercept_{660} = 0.32$) is nearly twice that for blue ($Intercept_{470} = 0.17$). But this time, slopes are much closer to unity than in the Aqua data with its value at red higher than at blue ($Slope_{470} = 0.77$, $Slope_{660} = 0.82$).

Correlation during Monsoon season is again much better at blue ($R^2_{470} = 0.46$, $R^2_{660} = 0.14$). Slope is higher and intercept is lower at blue than at red ($Slope_{470} = 0.71$, $Intercept_{470} = 0.20$; $Slope_{660} = 0.60$, $Intercept_{660} = 0.30$) - a feature in contrast to comparison from Aqua.

Post Monsoon season has the best correlation among all the cases both at blue ($R^2_{470} = 0.70$) as well as red ($R^2_{660} = 0.68$). Intercepts at both wavelengths have nearly similar values ($Intercept_{470} = 0.09$, $Intercept_{660} = 0.10$). Slope at red ($Slope_{660} = 0.66$) is better than at blue ($Slope_{470} = 0.59$) during this season.

These parameter values have been summarized in Table 5.2. Thus, except Monsoon season, for all the cases, slopes of correlation plot are higher at red than at blue. Intercepts are lower at blue than at red for all the seasons and lower at red for all the years except 2004. Except 2002, for all the cases, correlation is better at blue that at red. Among all the cases, Post Monsoon season has the best correlation whereas Dry season the least.

	470 nm			550 nm			660 nm		
Case	Slope	Intercept	R^2	Slope	Intercept	R^2	Slope	Intercept	R^2
Overall	0.54	0.16	0.35	0.57	0.18	0.28	0.76	0.16	0.25
2002	0.52	0.20	0.26	0.63	0.20	0.27	0.78	0.17	0.29
2003	0.54	0.17	0.40	0.57	0.17	0.33	0.78	0.12	0.29
2004	0.57	0.16	0.35	0.58	0.19	0.27	0.63	0.22	0.21
2005	0.57	0.12	0.39	0.68	0.12	0.27	1.04	0.07	0.26
Dry	0.39	0.17	0.32	0.39	0.19	0.19	0.47	0.19	0.10
Pre-Mon	0.77	0.17	0.46	0.76	0.25	0.45	0.82	0.32	0.40
Monsoon	0.71	0.20	0.46	0.60	0.27	0.28	0.60	0.30	0.14
Post-Mon	0.59	0.09	0.70	0.60	0.10	0.70	0.66	0.10	0.68

Table 5.2: Correlation Coefficients of Validation results of Terra C004 aerosol product

5.2 Validation results of the C005 Aerosol product

5.2.1 Aqua

In the updated product, for which the comparison plot has been shown in Figure 5.4a (for 470 nm), 5.4b (for 550 nm) and 5.4c (for 660 nm), the improvement in the correlation coefficient(R^2) is conspicuous in this and all other plots. The R^2 value is similar for both wavelengths(0.61 at blue and 0.69 at red) in the updated product. Another drastic improvement pertains to the intercept value which has dropped to 0.03 at blue and 0.003 at red [Misra et al., 2008]. As mentioned earlier, the intercept of the correlation plot denotes the errors due to inappropriate surface reflectance parameterization. Thus this improvement represents the successful modification of the surface reflectance ratios. Slope of the correlation is still better at red(0.80) than at blue(0.69), a feature still in contrast to [Levy et al., 2005]. Possibly it is because of the different aerosol types prevalent over the two study regions.

Comparison for different years

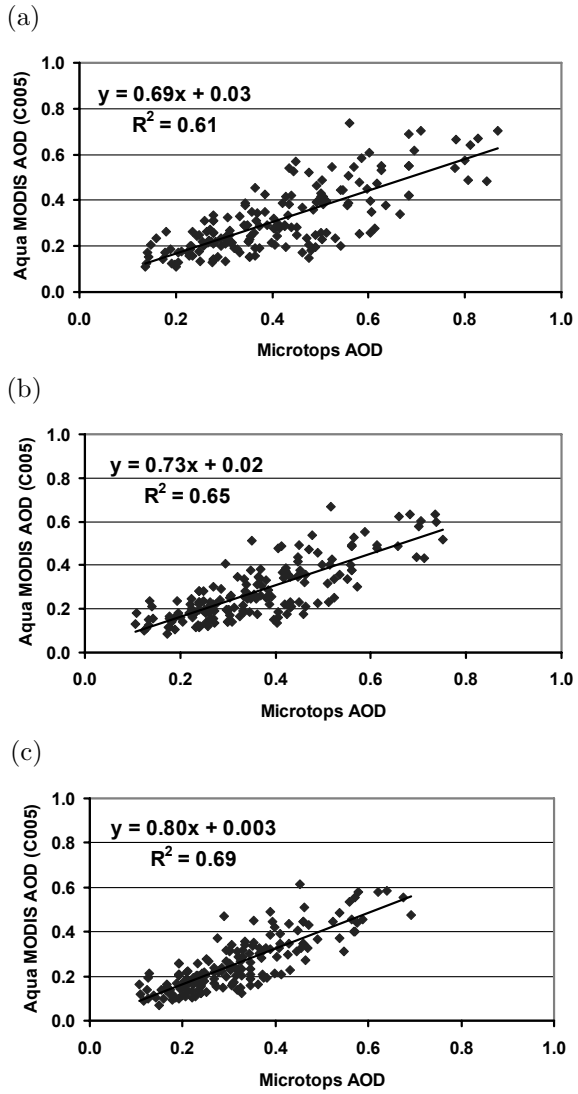

Figure 5.4: Validation results of the Aqua C005 aerosol product at (a)470 (b)550 and (c)660 nm

For 2002, the same pattern in slopes as observed in the C004 data is seen in the updated aerosol product also (Table 5.3) where slope at blue(0.77) is marginally higher than at red(0.70). But in every way, the updated product has a better correlation than the previous version. This shows that the AOD retrieval by MODIS at the two wavelengths depends on the surface reflectance and the dominant aerosol species for the particular case. As noted previously, 2002 was the year receiving the least rainfall.

In the updated product for 2003, slopes are higher and intercepts lower for red ($Slope_{660}$=0.82, $Intercept_{660}$ = −0.003, $Slope_{470}$=0.68, $Intercept_{470}$=0.03) whereas the correlation coefficient has shown more improvement at red (R^2_{660} =0.62, R^2_{470}=0.52). The negative intercept at red denotes over-correction for surface reflectance part.

For 2004, the slope is marginally larger and correlation coefficient higher

for red ($Slope_{660} = 0.71$, $R^2_{660} = 0.68$, $Slope_{470} = 0.68$, $R^2_{470} = 0.57$). However, intercepts are same at both the wavelengths($Intercept_{470}$=$Intercept_{660}$=0.03).

The updated product (C005) for 2005 has the best correlation among all the comparisons. The slope at red (0.9) is the closest approach to unity. The slope at blue (0.78), though not at par with that at red, is still quite larger as compared to other years. The intercepts for this year are the lowest among all the cases though their negative values denote an over-correction for the surface reflectance contribution. The correlation coefficients are also the best with its value at red(0.75) only marginally higher than at blue(0.71). 2005 was the year that received the highest amount of rainfall which increased the soil moisture content and greenness of surface thus reducing the surface reflectance part. This feature has been very well captured in the updated MODIS aerosol product. But the negative intercepts denote the over-correction for surface reflectance.

Comparison for different seasons

For Dry months, with the updated product, correlation shows substantial improvement at both the wavelengths and the new values of R^2 are nearly equal at both wavelengths(0.60 at blue and 0.62 at red). The slope, though much closer to unity than the previous version, is lower at blue than at red in the updated product also. Another noticeable feature is the reduction in the intercept values at both wavelengths being closer to zero at red than blue.

With the update to the C005 dataset, we see a great improvement in all the parameters during Pre Monsoon season. Slopes at both wavelengths are nearly equal with that at blue (0.84) only slightly higher than at red(0.81). Correlation coefficient is also highest during this season as compared to all other seasons, its value being 0.73 at blue and 0.81 at red. The extremely low values of intercept are also noteworthy(0.01 at blue and -0.0005 at red). In every regard, the updated MODIS aerosol product shows extremely good behaviour during Pre Monsoon months as compared to other seasons.

Similarly, upgrade to the C005 version improved the correlation coefficient during Monsoon also though its value at both wavelengths are still equal(0.65

	470 nm			550 nm			660 nm		
Case	Slope	Intercept	R^2	Slope	Intercept	R^2	Slope	Intercept	R^2
Overall	0.69	0.03	0.61	0.73	0.02	0.65	0.80	0.003	0.69
2002	0.77	0.05	0.51	0.76	0.06	0.53	0.70	0.05	0.56
2003	0.68	0.03	0.52	0.70	0.03	0.55	0.82	-0.003	0.62
2004	0.68	0.03	0.57	0.70	0.02	0.64	0.71	0.03	0.68
2005	0.78	-0.0002	0.71	0.84	-0.02	0.76	0.90	-0.03	0.75
Dry	0.65	0.04	0.60	0.70	0.03	0.59	0.83	0.004	0.62
Pre-Mon	0.84	0.01	0.73	0.82	0.003	0.78	0.81	-0.0005	0.81
Monsoon	0.87	0.03	0.65	0.80	0.06	0.63	0.82	0.03	0.62
Post-Mon	0.72	-0.03	0.66	0.77	-0.04	0.70	0.86	-0.05	0.71

Table 5.3: Correlation Coefficients of Validation results of Aqua C005 aerosol product

at blue and 0.62 at red). Intercepts in the new product are exactly equal at both wavelengths(0.03) and are higher than the Pre Monsoon values. The slope at blue(0.87) and red(0.82) are very close to their Pre Monsoon values.

For Post Monsoon season, the intercepts have negative values at both wavelengths(-0.03 at blue and -0.05 at red) representing an over-correction for the surface reflectance. The slope as well as correlation coefficient is higher at red (slope=0.86, R^2=0.71) than at blue(slope=0.72, R^2= 0.66).

These points have been depicted in Table 5.3. From the parameter values given there and the foregoing discussion, few features can be noticed. For the updated product, except 2002, slopes are better at red than blue for all the years as well as the combined data. Correlation coefficient is better at red for all the years whereas the intercept is either lower at red than blue or equal at both the wavelengths.

For the updated product(version C005), the best correlation is for 2005 with R^2 and slope highest and intercept lowest. This was the year receiving maximum rainfall so that soil moisture and increased vegetation led to reduced surface reflectance and hence to lower errors due to surface reflectance. Except monsoon season, the pattern of slope is preserved with the transition from C004 to C005 product viz, whenever the slope at blue was higher than at red for C004, it is the same case with C005 also and vice versa.

Interestingly, a comparative view of the slopes in the validation results (of the updated product) for different seasons at the two wavelengths reveals that the AOD is underestimated at 470 nm to a greater extent than 660 nm during Dry and Post Monsoon seasons. It may be recalled that during these seasons, the total aerosol content in the atmosphere is dominated by fine particles. The number concentration of the fine particles used in the look-up tables for aerosol retrieval by MODIS is lower than the actual content in the atmosphere during this season. Similarly, as noted earlier, during Pre-Monsoon and Monsoon months, the total aerosol content is dominated by coarse mode particles. During these months, it is observed that the AOD at 660 nm is more underestimated, though marginally, than at 470 nm. The number concentration of coarse particles during these seasons are not properly accounted for in the MODIS aerosol models and the actual coarse aerosol content is higher. Overall, the slopes differing from unity reflect the discrepancy between the aerosol models used in the MODIS aerosol retrieval scheme and the actual aerosol model. Further, the variation of slopes with season at the two wavelengths, especially corresponding to the dominant species present(smaller particles during Dry and Post Monsoon months and coarse particles during Pre-Monsoon and Monsoon months) implies that the aerosol model used by MODIS algorithm is not able to account for the seasonal variations in the aerosol type. This aspect forms the most important conclusion of our work [Misra et al., 2008].

The intercepts in the updated product for all seasons are less than 0.04 which is a great improvement over the previous version(C004) of the MODIS aerosol product and denotes a much better account of surface reflectance parameterization. The negative intercepts during Post Monsoon season, when the surface reflectance value itself is low, imply an over-correction for surface reflectance contribution.

Overall, the updated product has the best correlation for Pre-Monsoon among all seasons and Dry season the least.

5.2.2 Terra

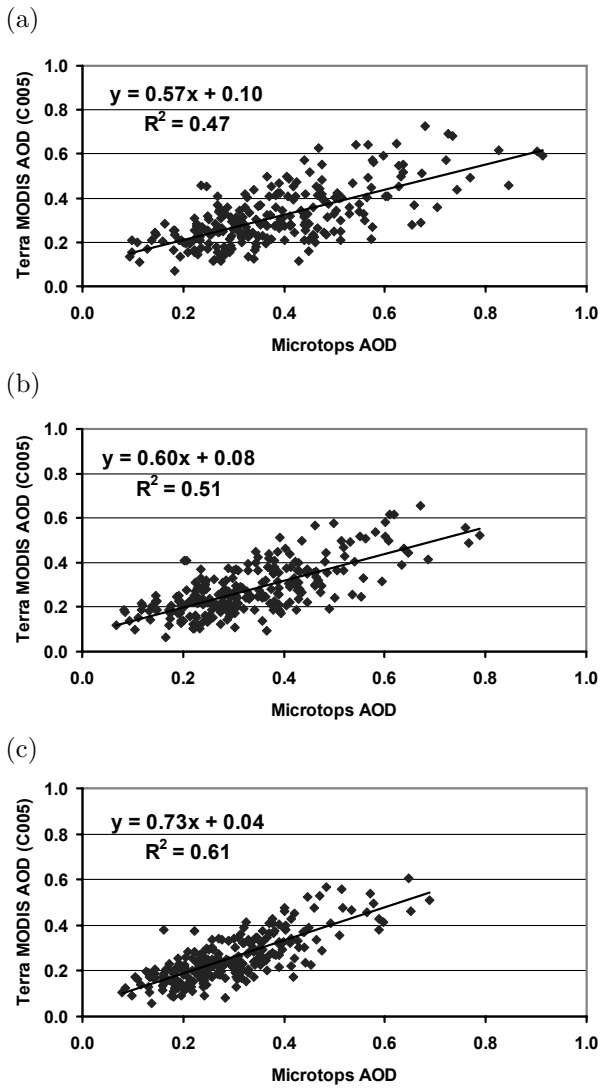

Figure 5.5: Validation Results of the MODIS aerosol product from Collection Version C005 from the Terra platform at (a)470 (b)550 (c)660 nm

Similar improvement in the correlation with upgrade to Collection Version C005 is seen in the validation results of Terra MODIS. Figure 5.5 shows the comparison of Collection Version C005 algorithm derived AOD values from Terra platform with the corresponding values from the ground based Microtops sunphotometer. A noticeable feature is the improvement in the correlation coefficient at red (R^2_{660} = 0.61) over the corresponding value from C004 algorithm. Correlation has also improved at blue wavelength (R^2_{470} = 0.47). Slope is still higher at red ($Slope_{660}$ = 0.73) than at blue ($Slope_{470}$ = 0.57) whereas the intercepts have reduced to a great extent from their C004 values with greater reduction in the red ($Intercept_{470}$ = 0.10, $Intercept_{660}$ = 0.04). Similar improvements in correlation are seen in nearly all the individual cases signifying a better parameterization of

surface reflectance and usage of aerosol models in the updated algorithm.

Comparison for different years

Similar to the C004 data during 2002, we see higher slope and correlation coefficient and lower intercept at red ($Slope_{660} = 0.60$, $Intercept_{660} = 0.10$, $R^2_{660} = 0.55$) than blue ($Slope_{470} = 0.41$, $Intercept_{470} = 0.18$, $R^2_{470} = 0.34$) in the updated product also. The improvement in the correlation at red wavelength is noticeable.

During 2003, not much improvement is noted at blue ($Slope_{470} = 0.56$, $Intercept_{470} = 0.11$, $R^2_{470} = 0.46$). Although, slope at red ($Slope_{660} = 0.66$) has reduced from its C004 value and intercept ($Intercept_{660} = 0.07$) has slightly improved from its C004 value, the major highlight of comparison for this year still remains the improvement in correlation especially at red ($R^2_{660} = 0.54$).

A tremendous improvement in all parameters of correlation plot is observed during 2004 at both wavelengths, where the slopes ($Slope_{470} = 0.74$, $Slope_{660} = 0.86$) and correlation coefficients ($R^2_{470} = 0.58$, $R^2_{660} = 0.76$) at both wavelengths are the highest among all the years. A considerable reduction is seen in the intercept values as well ($Intercept_{470} = 0.05$, $Intercept_{660} = 0.02$).

As noted previously, 2005 was the year receiving the maximum rainfall. This feature is again reflected in the intercept values of the comparison for this year which are the lowest among all the years ($Intercept_{470} = 0.03$, $Intercept_{660} = 0.003$). Both slope and correlation have improved at blue from the corresponding C004 values ($Slope_{470} = 0.61$, $R^2_{470} = 0.60$). Although the slope at red ($Slope_{660} = 0.73$) has reduced from its C004 value, the correlation coefficient has more than doubled ($R^2_{660} = 0.66$).

Comparison for different seasons

During Dry months, slope is closer to unity at red ($Slope_{660} = 0.70$) than at blue ($Slope_{470} = 0.54$) and intercept is also lower at red ($Intercept_{470} = 0.09$, $Intercept_{660} = 0.05$). Considerable improvement is observed in correlation

	470 nm			550 nm			660 nm		
Case	Slope	Intercept	R^2	Slope	Intercept	R^2	Slope	Intercept	R^2
Overall	0.57	0.10	0.47	0.60	0.08	0.51	0.73	0.04	0.61
2002	0.41	0.18	0.34	0.48	0.14	0.41	0.60	0.10	0.55
2003	0.56	0.11	0.46	0.55	0.10	0.46	0.66	0.07	0.54
2004	0.74	0.05	0.58	0.80	0.02	0.67	0.86	0.02	0.76
2005	0.61	0.03	0.60	0.65	0.01	0.63	0.73	0.003	0.66
Dry	0.54	0.09	0.50	0.57	0.08	0.49	0.70	0.05	0.53
Pre-Mon	0.71	0.11	0.49	0.66	0.10	0.50	0.72	0.07	0.60
Monsoon	0.94	0.03	0.68	0.79	0.08	0.66	0.86	0.04	0.72
Post-Mon	0.66	0.01	0.60	0.67	0.02	0.62	0.77	0.0002	0.69

Table 5.4: Correlation Coefficients of Validation results of Terra C005 aerosol product

coefficients from the C004 values at both wavelengths ($R^2_{470} = 0.50$, $R^2_{660} = 0.53$), the improvement being more at red.

Slopes at both wavelengths during Pre Monsoon season have nearly equal values ($Slope_{470} = 0.71$, $Slope_{660} = 0.72$). The correlation coefficient is higher and intercept lower at blue than at red ($Intercept_{470} = 0.11$, $R^2_{470} = 0.49$; $Intercept_{660} = 0.07$, $R^2_{660} = 0.60$).

The best correlation is observed during Monsoon season at both wavelengths ($R^2_{470} = 0.68$, $R^2_{660} = 0.72$). Slope is also highest during Monsoon months among all the seasons ($Slope_{470} = 0.94$, $Slope_{660} = 0.86$). Intercepts at both wavelengths have nearly equal values ($Intercept_{470} = 0.03$, $Intercept_{660} = 0.04$).

Lowest intercepts are observed during the Post Monsoon months among all seasons ($Intercept_{470} = 0.01$, $Intercept_{660} = 0.0002$). Correlation coefficients are also high - second only to the Monsoon months ($R^2_{470} = 0.60$, $R^2_{660} = 0.69$). Slope at red ($Slope_{660} = 0.77$) is higher than that at blue ($Slope_{470} = 0.66$) in this updated version as well.

Overall, for all the years, slopes and correlation coefficients are higher and intercepts lower at red than at blue. Best correlation and highest slopes are observed during 2004 whereas intercepts are lowest during 2005. Intercept, which shows error due to surface reflectance parameterization, has lowest

value for 2005 in Aqua dataset as well - a feature related to the highest rainfall received during this year. Similar to the Aqua dataset, the pattern of slope is preserved in transition from C004 to C005 in Terra data as well viz, whenever the slope at red is higher than at blue, it is the same case in the updated product as well.

The inadequacy of the aerosol models used in the C005 algorithm is reiterated in the Terra dataset where the slopes at blue are more underestimated during Dry and Post Monsoon seasons when the overall aerosol climatology is dominated by smaller particles. Even though the slope at both wavelengths are nearly equal during Pre Monsoon season, during Monsoon season slope is underestimated to a larger extent at red than blue. This is the season when the atmosphere is dominated by larger particles. Thus, the variation in the value of slopes with season in the Terra C005 data corroborates the results derived from the Aqua C005 dataset regarding the inadequacy of the aerosol models used in the MODIS C005 algorithm. Behaviour of slopes during Pre Monsoon season vis-a-viz the corresponding values from Aqua data is a feature which needs further investigation.

5.3 Validation results of the Deep Blue Aerosol product(Aqua)

As mentioned previously, the Deep Blue algorithm has been proposed as an alternative retrieval scheme for aerosol remote sensing over brighter surfaces. Presently, the data product corresponding to the Deep Blue Algorithm is available only from Aqua platform. Validation of the data product corresponding to this algorithm has been carried out for the same study period and dataset as for the conventional product. It is of further interest to compare the validation result from this algorithm to that from the Aqua C005 version data. Such an exercise will provide information corresponding to the suitability of a particular algorithm for retrieval of aerosol optical depth over our study location. An additional advantage of the Deep Blue Algorithm is the aerosol optical depth information at four wavelengths viz., 412, 470, 550

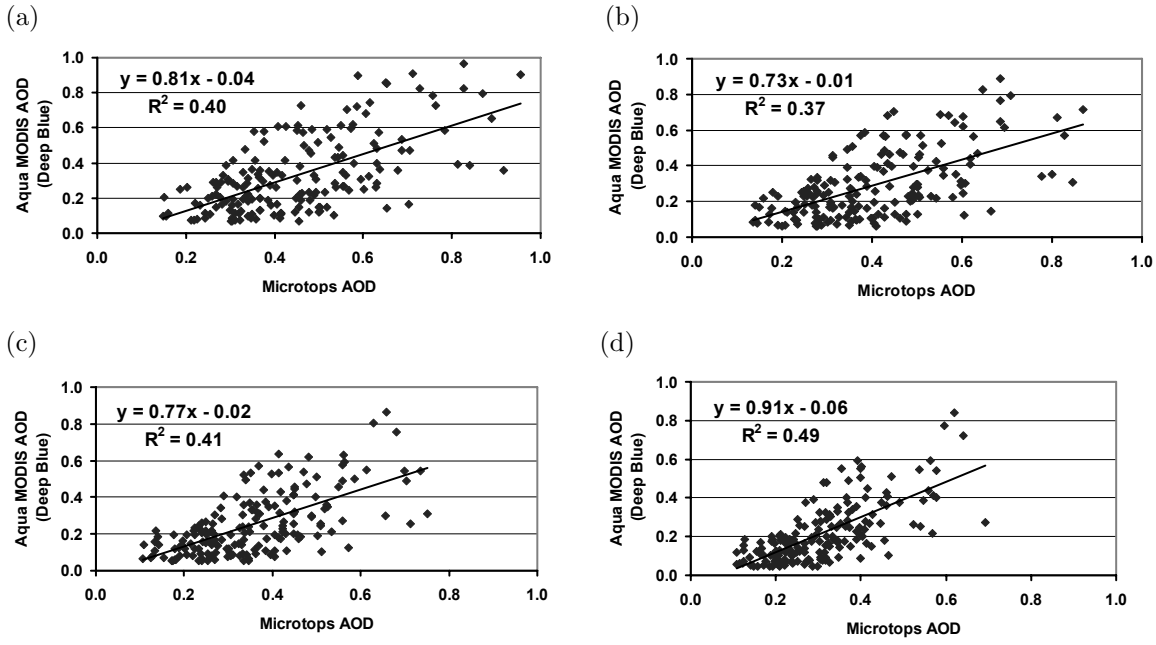

Figure 5.6: Validation results of the Aqua Deep Blue Algorithm aerosol product at (a)412 (b)470 (c)550 and (d)660 nm

and 660 nm. Here, AOD at 412, 470 and 660 nm are direct retrievals which are interpolated to get the AOD at 550 nm.

Figure 5.6 shows the validation results of the Deep Blue Algorithm derived aerosol optical depth from the Aqua platform. It is seen that intercepts are negative at all the wavelengths ($Intercept_{412}$= -0.04, $Intercept_{470}$= -0.01, $Intercept_{550}$= -0.02, $Intercept_{660}$= -0.06). Slope is closest to unity at 660 nm ($Slope_{660}$=0.91) and farthest at 470 nm ($Slope_{470}$= 0.73). The slopes at 412 and 550 nm lie within these two extremes ($Slope_{412}$= 0.81, $Slope_{550}$= 0.77). Correlation coefficient have the values R^2_{412} = 0.40, R^2_{470} = 0.37, R^2_{550} = 0.41 and R^2_{660}= 0.49 which shows that the correlation is much better for the retrieval from the C005 algorithm than the Deep Blue algorithm. In the following paragraphs we discuss features related to the Deep Blue algorithm validation for individual years and seasons. Since 412 nm retrieval is absent in the conventional algorithm and 550 nm retrieval is an interpolated value from the other direct retrievals of the Deep Blue algorithm, we limit our discussion

to 470 and 660 nm to be consistent with earlier discussion and to have a comparative view of the validation results from the different algorithms.

However, Table 5.5 reports the values of all the parameters of correlation for individual years and seasons for all the four wavelengths.

Comparison for different years

For 2002, the correlation (R^2_{470} = 0.22, R^2_{660} = 0.36) is poor as compared to that from C005. Slope is higher and intercept lower at red ($Slope_{660}$ = 0.49, $Intercept_{660}$ = 0.03) as compared to blue ($Slope_{470}$ = 0.44, $Intercept_{470}$ =0.07).

The slope at red is extremely close to unity during 2003 ($Slope_{660}$ = 0.99), whereas its value at blue is also considerably higher ($Slope_{470}$ = 0.73). The correlation is better for red (R^2_{660} = 0.49) than blue (R^2_{470} = 0.31) and the value of intercept is also lower at this wavelength ($Intercept_{470}$ = 0.004, $Intercept_{660}$ = -0.10).

For 2004 also, the slope is higher at red ($Slope_{660}$ = 0.66) than at blue ($Slope_{470}$ = 0.46), the intercept is also lower and correlation better at red ($Intercept_{660}$ = 0.01, R^2_{660} = 0.34) than blue ($Intercept_{470}$ = 0.09, R^2_{470} = 0.17).

Same pattern is followed during 2005 as well when the slope is higher at red ($Slope_{660}$ = 1.11) than blue ($Slope_{470}$ = 0.94). Correlation coefficient is also higher at red (R^2_{470} = 0.45, R^2_{660} = 0.58). Intercepts at blue ($Intercept_{470}$ = -0.07) as well as red ($Intercept_{660}$ = -0.11) are negative.

Comparison for different seasons

During Dry season, slope at blue ($Slope_{470}$ = 0.83) is only marginally higher than that at red ($Slope_{660}$ = 0.81) and correlation coefficient is also nearly equal at both wavelengths (R^2_{470} = 0.52, R^2_{660} = 0.51). Values of intercept are negative and exactly equal at both red and blue ($Intercept_{470}$ = $Intercept_{660}$ = -0.04).

During Pre Monsoon season, the slope at red ($Slope_{660}$ = 1.29) is marginally higher than at blue ($Slope_{470}$ = 1.28), the values at both wavelengths being

greater than 1. Intercepts at both red and blue are negative for this season as well ($Intercept_{470}$ = -0.07, $Intercept_{660}$ = -0.09), whereas correlation coefficient is considerably high at both these wavelengths, its value at blue ($R^2_{470} = 0.80$) only slightly higher than at red ($R^2_{660} = 0.78$).

During Monsoon season, slope is much higher at red ($Slope_{660} = 0.93$) than blue ($Slope_{470} = 0.78$). The intercepts at both wavelengths are very low ($Intercept_{470} = 0.05$, $Intercept_{660}$ = -0.03), the value at red being negative. The correlation coefficient has lower value during Monsoon as compared to other seasons ($R^2_{470} = 0.32$, $R^2_{660} = 0.43$).

Intercepts are negative at both wavelengths during Post Monsoon season ($Intercept_{470}$ = -0.06, $Intercept_{660}$ = -0.03). The correlation coefficient as well as slope is higher at blue than at red ($Slope_{470} = 0.62$, $R^2_{470} = 0.47$; $Slope_{660} = 0.55$, $R^2_{660} = 0.45$) during this season.

These points have been summarized in Table 5.5. Comparing these validation results with those from the C005 product [Levy et al., 2007b] we find that at 470 nm, slopes are better for Deep Blue product during 2003 and 2005 as well as the overall plot, whereas during 2002 and 2004, slopes for C005 are better. Among seasons, during Dry and Pre Monsoon months, Deep Blue slopes are higher whereas C005 gives higher slopes during Monsoon and Post monsoon months. Intercept values for Deep Blue are higher than C005 during 2002 and 2004 and lower during 2003 and 2005. Negative intercept is observed during 2005 and also for all seasons except Monsoon. For all years and overall plot, R^2 values are better for C005. Among seasons, except Pre Monsoon months, R^2 values are better for C005 comparison.

At 660 nm, slopes have the same pattern as at 470 nm viz, better for Deep Blue during 2003 and 2005 but better for C005 during 2002 and 2004. Except Post Monsoon season, all seasons have slopes either nearly equal (Dry season) from both algorithms or higher for Deep Blue (Pre Monsoon and Monsoon). Correlation plots for all seasons show negative intercepts at 660 nm. Among years, intercepts for Deep Blue are less than C005, but slightly positive during 2002 and 2004 and negative during 2003 and 2005. R^2 values for all years and seasons are better for C005 comparison.

A comparative study of the correlations at the two wavelengths shows

that for all years and the overall plot, slope is better at 660 nm than 470 nm. Among seasons, slopes are nearly same for Dry and Pre Monsoon season, higher at 660 nm for Monsoon and at 470 nm during Post Monsoon season. For all years and the overall plot, R^2 at 660 nm is higher. Among seasons, R^2 is higher at 660 nm during Monsoon whereas during other seasons, R^2 at 470 nm is higher.

	412 nm			470 nm			550 nm			660 nm		
Case	Slope	Intercept	R^2	Slope	Intercept	R^2	Slope	Intercept	R^2	Slope	Intercept	R^2
Overall	0.81	-0.04	0.40	0.73	-0.01	0.37	0.77	-0.02	0.41	0.91	-0.06	0.49
2002	0.43	0.06	0.19	0.44	0.07	0.22	0.49	0.05	0.29	0.49	0.03	0.36
2003	0.93	-0.10	0.38	0.73	0.004	0.31	0.76	-0.02	0.35	0.99	-0.10	0.49
2004	0.44	0.11	0.15	0.46	0.09	0.17	0.56	0.04	0.24	0.66	0.01	0.34
2005	0.99	-0.09	0.45	0.94	-0.07	0.45	0.996	-0.09	0.50	1.11	-0.11	0.58
Dry	0.94	-0.09	0.58	0.83	-0.04	0.52	0.77	-0.02	0.49	0.81	-0.04	0.51
Pre-Mon	1.29	-0.07	0.78	1.28	-0.07	0.80	1.27	-0.08	0.80	1.29	-0.09	0.78
Monsoon	0.67	0.11	0.21	0.78	0.05	0.32	0.91	-0.002	0.43	0.93	-0.03	0.43
Post-Mon	0.72	-0.11	0.47	0.62	-0.06	0.47	0.57	-0.04	0.47	0.55	-0.03	0.45

Table 5.5: Correlation Coefficients of Validation results of Aqua Deep Blue aerosol product

Chapter 6

Validation Results for the ISRO-GBP Land Campaigns

Besides having an understanding of the accuracy of MODIS derived aerosol optical depth as validated from a fixed location covering a temporal period encompassing several years and seasons, it is necessary to validate the aerosol product at different geographical locations. Such an exercise aids in identifying the level upto which surface reflectance and aerosol model - which usually vary from place to place - affect the retrieval accuracy and to look into the possibility of better parameterization and account for these parameters. Such exercises have in the past, for example, led to the inclusion of Heavy Absorption aerosol model to be used in the MODIS over land algorithm [Ichoku et al., 2003] and the latest update to the MODIS algorithm leading to the Collection version C005 [Levy et al., 2005].

The two ISRO-GBP (Indian Space Research Organization- Geosphere Biosphere Programme) Land Campaigns provided opportunities to test the MODIS aerosol retrieval algorithms under varying environmental and surface conditions. The First ISRO-GBP Land Campaign was carried out in early 2004 to characterize the aerosol and trace gases distribution over peninsular India. The objective of the second ISRO-GBP land campaign - carried out in end of 2004 - was to understand the aerosol and trace gas distribution along the Indo-Gangetic plain under foggy conditions. In this chapter we discuss

in detail the results obtained from the validation of MODIS aerosol product under different environmental conditions during these two experiments.

6.1 Validation During the ISRO-GBP Land Campaign - I

In order to have a detailed information regarding the aerosol characteristics and trace gas amount over peninsular India, a field campaign experiment was carried out during 7 to 29 February 2004 between Ahmedabad (72.53E, 23.03N) and Hyderabad (78.27E, 17.28N) under the auspices of the Indian Space Research Organization - Geosphere Biosphere Program (ISRO-GBP). Measurements of various aerosol optical and physical properties were carried out using a variety of instruments such as Microtops sunphotometer, Quartz Crystal Microbalance, Grimm Particle Size Analyzer, Nephelometer, Aethalometer and the Micro Pulse Lidar. During the campaign period, a distance of ∼1200 Km was covered, taking observations every 120 Km. In order to avoid the effects of local sources, special care was taken to select the measurement sites which were preferably remote sites far from any industrial or traffic sources. The experimental trip is classified into three legs: onward journey between 7 and 14 February from Ahmedabad to Hyderabad, during 16 to 21 February intercomparison with the instruments from other institutes were carried out at Shadnagar (78.18E, 17.03N) and return journey from Hyderabad to Ahmedabad took place between 23 and 29 February. In order to see any possible temporal variation in the aerosol properties during the onward and return journey, attempts were made to make measurements at the same location in the return journey as were done during the onward trip [Jayaraman et al., 2006].

Measurements from the Microtops sunphotometer showed AOD values to increase by a factor of more than two during the onward trip which shows an increased total aerosol content. Study of the Angstrom exponent variation showed more surface-derived mineral aerosols in the northern stations as compared to the southern ones. A decrease in the value of α during the

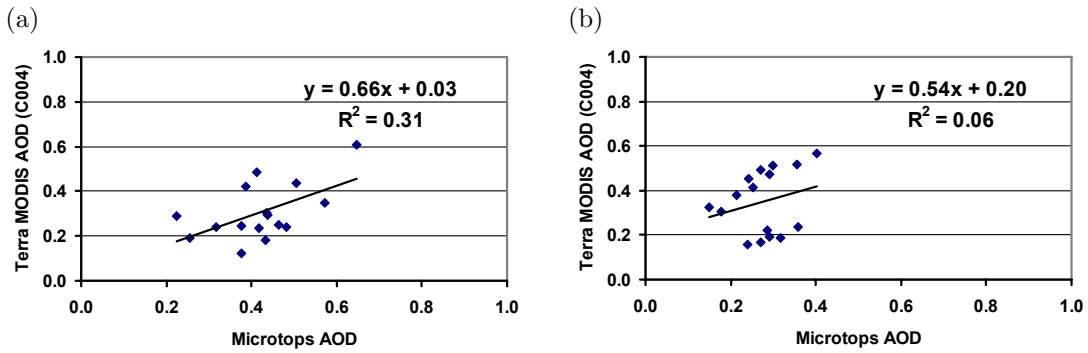

Figure 6.1: Validation results of Terra MODIS C004 aerosol optical depth during LC1 at (a) 470 and (b) 660 nm

return trip accompanied by an increase in β represented the increase in the coarse mineral particle with the change in season. Such behaviour was seen in the observation of aerosol scattering coefficient as well. Thus return jouney witnessed larger concentration of coarse particles. It is important to remember these variations in aerosol content and type during the onward and return journey for interpreting the validation results of the MODIS aerosol product [Jayaraman et al., 2006].

Though several observations were carried out at a particular station, there would be only one data corresponding to a single overpass by MODIS. Further, the overpass regions were quite heterogeneous in surface properties as well as in terms of the dominant aerosol type.

Table 6.1 gives the values of all parameters of correlation between the two sets of data. MODIS data from all the three algorithms and both satellite platforms are represented.

Terra C004

Validation results of MODIS Collection Version 4 AOD from Terra platform is shown in Figure 6.1. We see that the slopes are very less at both wavelengths ($Slope_{470} = 0.66$, $Slope_{660} = 0.54$). Correlation at red is extremely poor (R^2_{660} = 0.06) as compared to blue (R^2_{470} = 0.31) and also has a large intercept

($Intercept_{660} = 0.20$). Intercept at blue is comparatively better($Intercept_{470} = 0.03$).

As mentioned previously, the overall data consists of both the onward and return journey observations. The parameter values for individual legs of the journey are also indicated in Table 6.1. Values of slope and intercept at blue during onward journey ($Slope_{470} = 0.68$, $Intercept_{470} = 0.05$) is slightly higher than the overall comparison although the correlation is better ($R^2_{470} = 0.49$). At red, intercept during onward journey is even higher ($Intercept_{660} = 0.27$) and slope lower ($Slope_{660} = 0.40$) than the whole trip. The correlation at this wavelength ($R^2_{660} = 0.08$) is still extremely poor.

Correlation at red is considerably better during return journey ($R^2_{660} = 0.75$) and slope is also closer to unity ($Slope_{660} = 0.97$). But the intercept is still very large ($Intercept_{660} = 0.19$). But this time, the correlation at blue wavelength is poor ($R^2_{470} = 0.04$) with large intercept ($Intercept_{470} = 0.22$) and low value of slope ($Slope_{470} = 0.32$) as compared to both the onward journey as well as the overall trip.

Thus the validation of Terra MODIS Collection Version C004 data shows better correlation at blue during onward trip and at red during return trip.

Aqua C004

Overall correlation of Aqua MODIS C004 data with sunphotometer is poorer as compared to that for Terra at both wavelengths ($R^2_{470} = 0.09$, $R^2_{660} = 0.05$). The correlation at red is nearly similar to that for data from Terra. Slope at this wavelength is moderate ($Slope_{660} = 0.48$) and intercept is large ($Intercept_{660} = 0.25$). Intercept at blue though lower than at red, is still quite large whereas the slope is extremely low (($Slope_{470} = 0.21$, $Intercept_{470} = 0.20$)).

Slope as well as correlation coefficient show considerable improvement at blue during onward trip ($Slope_{470} = 0.67$, $R^2_{470} = 0.72$) and the value of intercept also reduces greatly from its value for overall trip ($Intercept_{470} = 0.09$). But the correlation, though better than the overall trip, is still not good ($Slope_{660} = 1.12$, $Intercept_{660} = 0.15$, $R^2_{660} = 0.24$). Thus the better

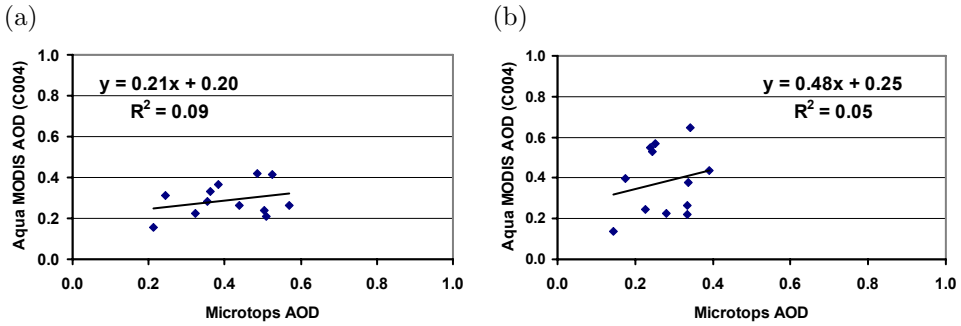

Figure 6.2: Validation results of Aqua MODIS C004 aerosol optical depth during LC1 at (a) 470 and (b) 660 nm

correlation at blue wavelength during onward trip as seen in the Terra dataset is reflected in the data from Aqua as well.

Correlation is once again poor at blue during return trip as in the Terra dataset ($Slope_{470} = 0.27$, $Intercept_{470} = 0.18$, $R^2_{470} = 0.13$). The slope at red during this leg retains its high value ($Slope_{660} = 0.95$) though correlation at this wavelength has not improved ($R^2_{660} = 0.19$). Thus the better correlation at red in the Terra data during return trip is not seen in the Aqua dataset.

Terra C005

With the upgrade to the Collection Version C005, we notice a tremendous improvement in all correlation parameters at both wavelengths. The intercepts at both red and blue are equal and negative ($Intercept_{470} = Intercept_{660}$ = -0.01). Overall correlation is better at blue than red ($R^2_{470} = 0.61$, R^2_{660} = 0.53) whereas slope is closer to unity at red than blue ($Slope_{470} = 0.76$, $Slope_{660} = 0.94$).

Intercepts are nearly equal at both wavelengths during onward journey ($Intercept_{470} = 0.02$, $Intercept_{660} = 0.01$) and as in the case of C004 validation, better correlation at blue during onward trip is seen in the Terra C005 dataset as well ($R^2_{470} = 0.86$, $R^2_{660} = 0.67$). An interesting feature is seen in the slopes of the correlation plot. We find that the slope at red is closer to unity than blue ($Slope_{470} = 0.74$, $Slope_{660} = 0.92$), or in other

words, during onward trip, AOD at blue is underestimated to a greater extent than at red. As noted previously, aerosol climatology during onward journey witnessed less amount of coarse particles. This feature pointing towards the inadequacy of aerosol model is similar to the results from study over Ahmedabad.

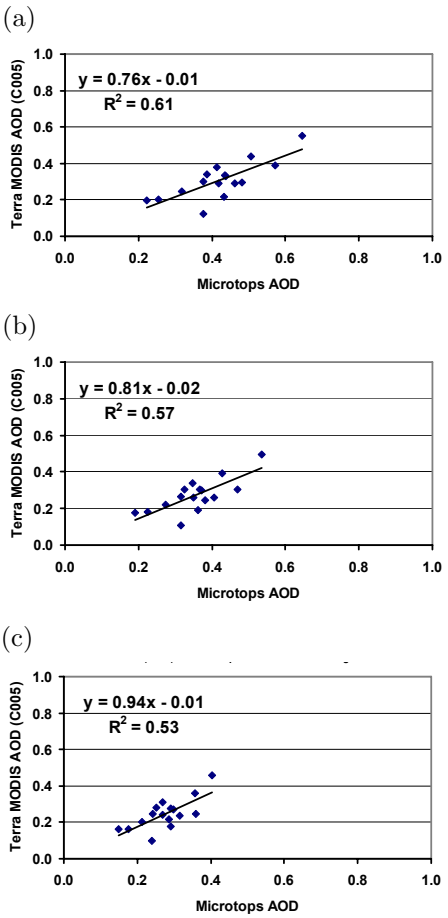

Figure 6.3: Validation results of Terra MODIS C005 aerosol optical depth during LC1 at (a) 470, (b) 550 (c) 660 nm

This fact is further reinforced in the slope values during return trip where we see the underestimation to be more at red than blue ($Slope_{470}$ = 0.88, $Slope_{660}$ = 0.84). During return leg, the coarse particles were in larger amount so that this underestimation at longer wavelength indicates the lesser amount of coarse particles in the aerosol model used by the retrieval algorithm. Correlation is good at both the wavelengths (R^2_{470} = 0.72, R^2_{660} = 0.73) and the intercepts are also low ($Intercept_{470}$ = -0.03, $Intercept_{660}$ = 0.05).

Aqua C005

Although the correlation has improved with upgrade to C005 in Aqua dataset also, it is still poor (R^2_{470} = 0.16, R^2_{660} = 0.13) as compared to the Terra case. Intercepts are

large ($Intercept_{470}$ = 0.13, $Intercept_{660}$ = 0.11) and slopes low at both red and blue ($Slope_{470}$ = 0.295, $Slope_{660}$ = 0.35).

(a)

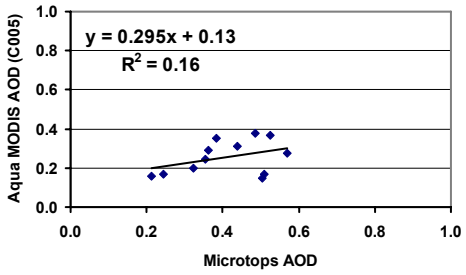

(b)

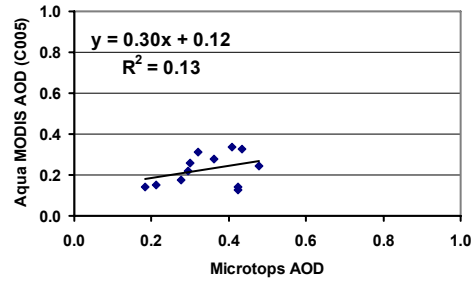

(c)

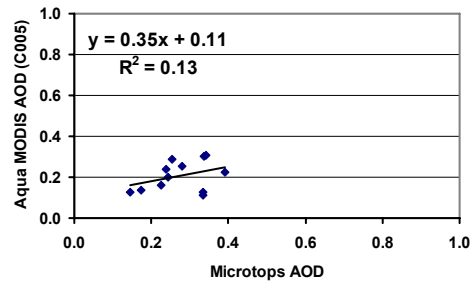

Figure 6.4: Validation results of Aqua MODIS C005 aerosol optical depth during LC1 at (a) 470 nm, (b) 550 and (a) 660 nm

Correlation is found to be good during onward journey and correlation coefficient has equal value at both wavelengths ($R^2_{470} = R^2_{660}$ = 0.87). Intercepts are also seen to be very low ($Intercept_{470}$ = 0.01, $Intercept_{660}$ = -0.01). Again we see the underestimation to be larger at blue wavelength ($Slope_{470}$ = 0.74) showing lesser amount of smaller particles in the MODIS aerosol models used by MODIS algorithm. The slope at red is nearly equal to unity ($Slope_{660}$ = 1.005).

As compared to the onward trip, correlation is inferior during return trip and is presumably responsible for poor correlation of the overall comparison (R^2_{470} = 0.39, R^2_{660} = 0.42) though the improvement from the corresponding values in C004 data is noteworthy. Intercepts are low showing reduced error due to surface reflectance ($Intercept_{470}$ = 0.096, $Intercept_{660}$ = 0.07). But slopes in this dataset are not in accordance to the feature observed in Terra dataset and the onward journey of the Aqua C005 ($Slope_{470}$ = 0.41, $Slope_{660}$ = 0.51).

Since the aerosol climatology is dominated by coarse particles, we expect the underestimation to be more at red than blue as shown by the validation results from Ahmedabad studies and those from Terra C005 of this experiment. This aspect requires further investigation.

Aqua C005 (Deep Blue Algorithm)

Although Deep Blue algorithm provides additional retrieval in 412 nm, this is not included in the discussion for consistency with other algorithms. However the parameters related to the validation of this algorithm are provided in Table 6.1. The overall correlation for Aqua Deep Blue aerosol product is better than Aqua C005 at both red and blue (R^2_{470} = 0.54, R^2_{660} = 0.49). Intercepts are low and have negative values at all wavelengths ($Intercept_{470}$ = -0.05, $Intercept_{660}$ = -0.008). Values of slopes are also higher as compared to Aqua C005, the value at blue being greater than at red ($Slope_{470}$ = 0.74, $Slope_{660}$ = 0.65).

Intercepts are negative during onward trip also ($Intercept_{470}$ = -0.14, $Intercept_{660}$ = -0.07), but the correlation is better than the overall correlation at both wavelengths (R^2_{470} = 0.78, R^2_{660} = 0.71). Values of slopes are high being closer to unity at blue than red ($Slope_{470}$ = 0.95, $Slope_{660}$ = 0.87).

However, during the return trip slope is low and intercept is large at red ($Slope_{660}$ = 0.30, $Intercept_{660}$ = 0.12) as compared to the values during onward trip. The value of correlation coefficient at this wavelength (R^2_{660} = 0.33) is lower than that for Aqua C005. The corresponding values at blue are comparatively better ($Slope_{470}$ = 0.51, $Intercept_{470}$ = 0.08, R^2_{470} = 0.71).

Overall, in the case of Deep Blue algorithm, the comparison is better at blue than red.

	412 nm			470 nm			550 nm			660 nm		
	Sl	In	R^2	Sl	In	R^2	Sl	In	R^2	Sl	In	R^2
Aqua MODIS Collection Version C004												
W				0.21	0.20	0.09				0.48	0.25	0.05
O				0.67	0.09	0.72				1.12	0.15	0.24
R				0.27	0.18	0.13				0.95	0.18	0.19
Terra MODIS Collection Version C004												
W				0.66	0.03	0.31				0.54	0.20	0.06
O				0.68	0.05	0.49				0.40	0.27	0.08
R				0.32	0.22	0.04				0.97	0.19	0.75
Aqua MODIS Collection Version C005												
W				0.295	0.13	0.16	0.30	0.12	0.13	0.35	0.11	0.13
O				0.74	0.01	0.87	0.83	-0.003	0.86	1.005	-0.01	0.87
R				0.41	0.096	0.39	0.44	0.08	0.38	0.51	0.07	0.42
Terra MODIS Collection Version C005												
W				0.76	-0.01	0.61	0.81	-0.02	0.57	0.94	-0.01	0.53
O				0.74	0.02	0.86	0.78	0.01	0.77	0.92	0.01	0.67
R				0.88	-0.03	0.72	0.89	-0.006	0.71	0.84	0.05	0.73
Aqua MODIS Deep Blue Algorithm												
W	0.81	-0.08	0.55	0.74	-0.05	0.54	0.68	-0.03	0.51	0.65	-0.008	0.49
O	0.999	-0.17	0.76	0.95	-0.14	0.78	0.91	-0.11	0.76	0.87	-0.07	0.71
R	0.63	0.04	0.82	0.51	0.08	0.71	0.398	0.11	0.51	0.30	0.12	0.33

Table 6.1: Values of parameters of correlation between various MODIS aerosol optical products and the Microtops sunphotometer derived aerosol optical depth during the First ISRO GBP Land Campaign. W = Whole Journey, O = Onward Trip, R = Return Trip

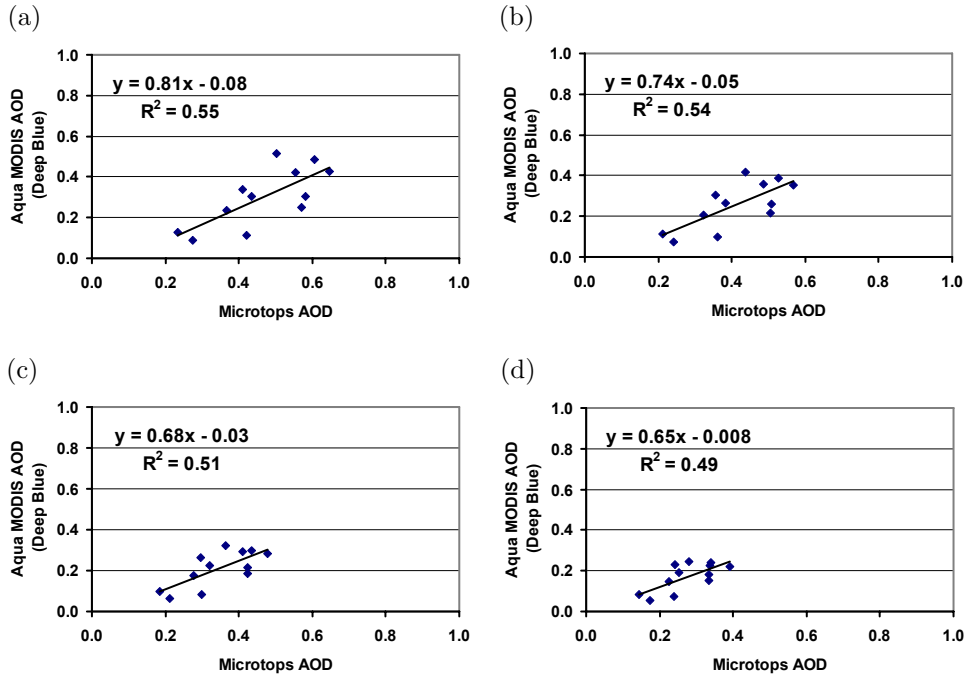

Figure 6.5: Validation results of Aqua Deep Blue aerosol optical depth for LC1 at (a) 412 (b) 470 (c) 550 and (d) 660 nm

6.2 Validation During the ISRO-GBP Land Campaign - II

The second ISRO-GBP Land Campaign was carried out during December 2004 along the Indo-Gangetic Plain. This region during the winter season experience extremely low temperature and high humidity alongwith low wind speed resulting in the formation of fog. The objective of the experiment was to study the ditribution of aerosol, their physical, optical and chemical characteristics and transport processes. Further, knowledge about the aerosol properties during high humidity conditions, their role in formation of fog and the aerosol fog interaction were sought. Together these results provide a better understanding of the aerosol impact on fog formation and aerosol radiative forcing under hazy environment.

MODIS retrieved aerosol optical depth from the three algorithm are com-

pared with the ground based Microtops sunphotometer observations over Delhi (77.17E, 28.63N) for the campaign period of 1 to 31 December 2004 as part of this campaign. Validation exercise in such campaign mode has the advantage of having a larger volume of data so that possiblity of having sunphotometer measurement closer to the MODIS overpass increases. Measurements of aerosol optical depth from Microtops sunphotometer were made at an interval of half an hour. At each instant, three measurements were made and the one giving lowest value of aerosol optical depth was selected. This way any possiblity of cloud contamination is minimized.

To aid further analysis, the campaign period was classified into three categories viz., clear, foggy and hazy days based on the visibility and meterological parameters. Wind speed was low during this period whereas relative humidity showed high vlaues with large variations. Overall temperatures were very low as noted previously. The lower wind speeds also result in lesser amount of surface derived coarse particles so that the overall climatology during the experiment was dominated by anthropogenic particles [Ganguly et al., 2006b].

Terra C004

The validation result of Terra MODIS C004 aerosol product is shown in refterrac004lc2. Here we see that the slopes of the correlation plots at both red and blue are very low ($Slope_{470} = 0.22$, $Slope_{660} = 0.21$). Further, intercepts are also very large ($Intercept_{470} = 0.31$, $Intercept_{660} = 0.28$) at both these wavelengths. The above case includes data for all days. Excluding the data from hazy and foggy days, increases the slopes to ($Slope_{470} = 0.54$, $Slope_{660} = 0.48$) and reduces the values of intercepts ($Intercept_{470} = 0.10$, $Intercept_{660} = 0.16$). The correlation coefficients increase from ($R^2_{470} = 0.35$, $R^2_{660} = 0.33$) in the case of all-days plot to ($R^2_{470} = 0.59$, $R^2_{660} = 0.52$) for clear days.

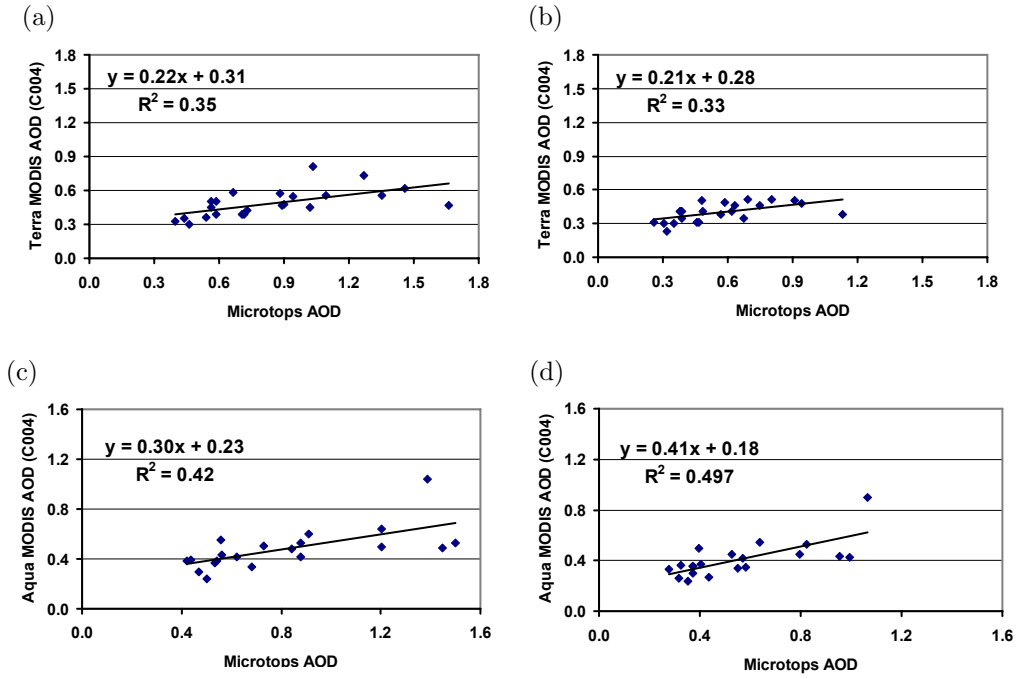

Figure 6.6: Validation results of MODIS C004 aerosol optical depth from Terra at (a) 470 (b) 660 nm and Aqua at (c) 470 and (d) 660 nm during LC2

Aqua C004

Similar poor correlatation is seen in the validation of the Aqua MODIS C004 product also. Here the slope is larger and intercept lower at red ($Slope_{660}$ = 0.41, $Intercept_{660}$ = 0.18) than at blue ($Slope_{470}$ = 0.30, $Intercept_{470}$ = 0.23). The correlation coefficient has higher value at red (R^2_{470} = 0.42, R^2_{660} = 0.497). Considering only clear days deteriorates the correlation at both wavelengths ($Slope_{470}$ = 0.24, $Intercept_{470}$ = 0.26, R^2_{470} = 0.17; $Slope_{660}$ = 0.198, $Intercept_{660}$ = 0.27, R^2_{660} = 0.07).

Terra C005

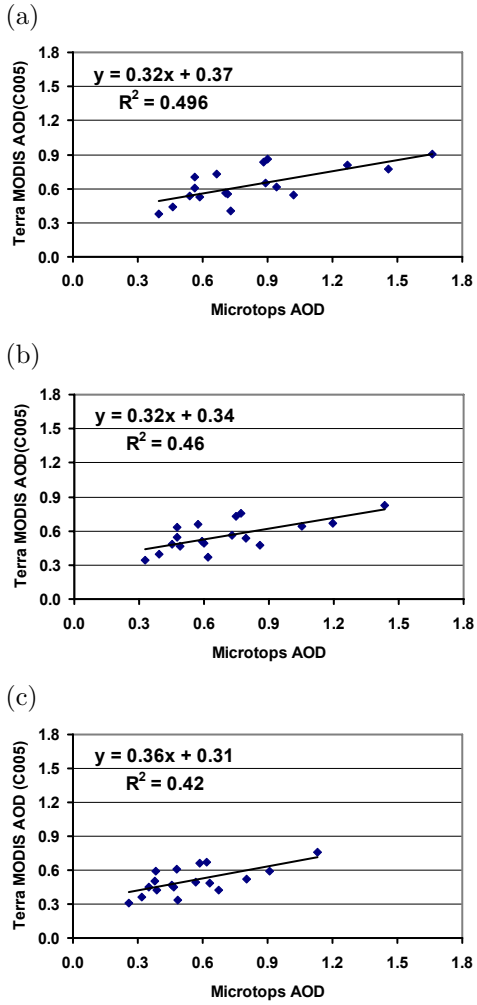

Figure 6.7: Validation results of MODIS C005 aerosol optical depth from Terra at (a) 470 (b) 550 nm and (c) 660 nm

Upgrade to the Collection Version C005 only slightly improves the correlation for Terra MODIS dataset from its C004 values (R^2_{470} = 0.496, R^2_{660} = 0.42). Though the values of slopes at both red and blue have increased ($Slope_{470}$ = 0.32, $Slope_{660}$ = 0.36), the values of intercepts also have increased ($Intercept_{470}$ = 0.37, $Intercept_{660}$ = 0.31). Considering only clear days does not improve the correlation at red (R^2_{660} = 0.42) but increase the correlation coefficient at blue by a small amount(R^2_{470} = 0.49). Intercepts also reduce at both the wavelengths in case of clear days validation ($Intercept_{470}$ = 0.30, $Intercept_{660}$ = 0.26). An interesting feature is seen regarding slopes of the correlation plot. We see that the underestimation is larger at blue than red ($Slope_{470}$ = 0.398, $Slope_{660}$ = 0.46). As noted previously, the aerosol climatology during the season when this campain was carried out is dominated by smaller particles. Thus, this behaviour of slopes of correlation plots shows that the amount of smaller particles in the aerosol models used by MODIS algorithm

is less.

Aqua C005

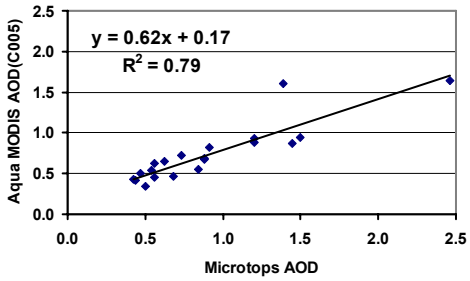

(a)

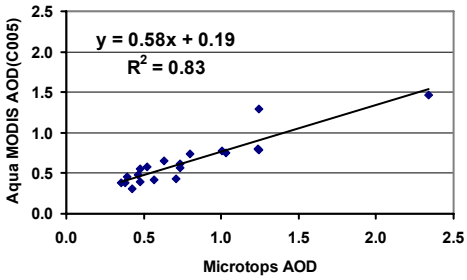

(b)

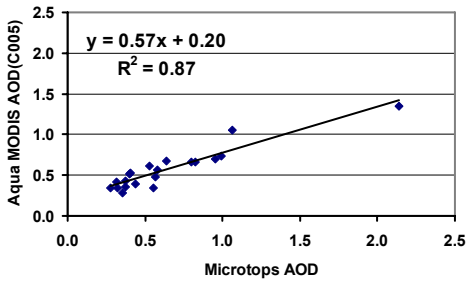

(c)

Figure 6.8: Validation results of Aqua at (a) 470 (b) 550 and (a) 660 nm during LC2

the MODIS aerosol models.

Considerable improvement is noticed in correlation of Aqua MODIS dataset with upgrade to Collection Version C005 (R^2_{470} = 0.79, R^2_{660} = 0.87). Similar improvement is noted in the slopes as well ($Slope_{470}$ = 0.62, $Slope_{660}$ = 0.57), although the intercepts at both red and blue have large values ($Intercept_{470}$ = 0.17, $Intercept_{660}$ = 0.20). Considering only the clear days reduces the correlation at both red and blue (R^2_{470} = 0.42, R^2_{660} = 0.29). Intercept at red ($Intercept_{660}$ = 0.19) remain nearly unaffected whereas that at blue increases ($Intercept_{470}$ = 0.23). Similar to the Terra C005 dataset, the slope at blue is underestimated to a greater extent than at red($Slope_{470}$ = 0.499, $Slope_{660}$ = 0.57), thus indicating the insufficient amount of smaller particles in

Aqua C005 (Deep Blue Algorithm)

The Deep Blue algorithm derived aerosol optical depth values show good correlation with sunphotometer values at both red and blue ($R^2_{470} = 0.79$, $R^2_{660} = 0.80$). The values of intercepts are lower than other algorithms ($Intercept_{470}$ = -0.02, $Intercept_{660} = 0.09$). Slope is nearly unity at blue ($Slope_{470} = 1.04$) whereas that at red is much less than unity ($Slope_{660} = 0.69$). Considering only clear days does not affect the correlation at either wavelength ($R^2_{470} = 0.79$, $R^2_{660} = 0.798$). But slopes have increased in value at both red and blue ($Slope_{470} = 1.48$, $Slope_{660} = 1.31$). These features are summarized in Table 6.2

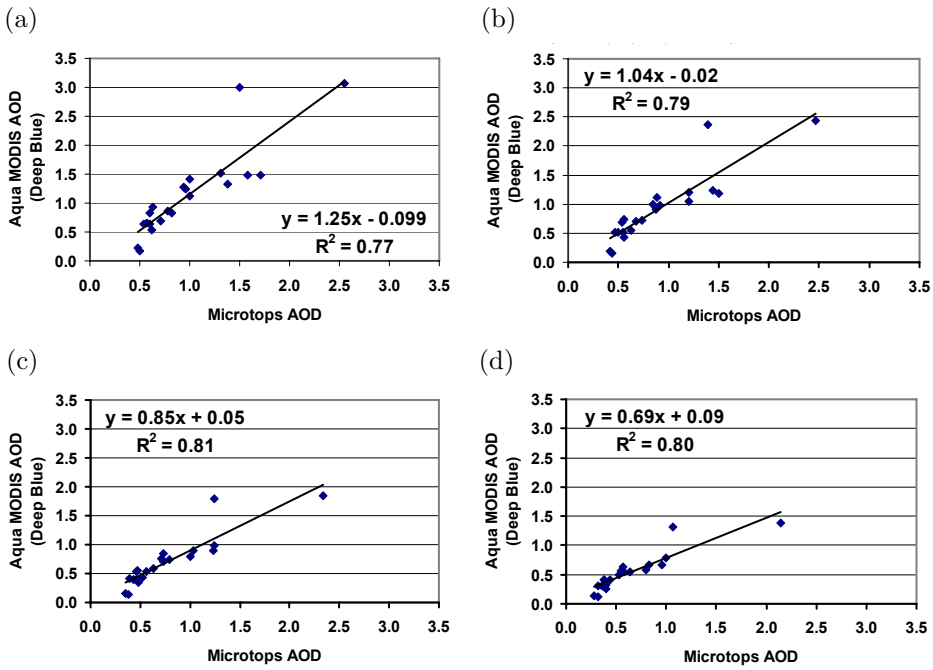

Figure 6.9: Validation results of the Aqua Deep Blue algorithm aerosol optical depth at (a) 412 (b) 470 (c) 550 and (d) 660 nm during LC2

	412 nm			470 nm			550 nm			660 nm		
Case	Sl	In	R^2	Sl	In	R^2	Sl	In	R^2	Sl	In	R^2
Aqua MODIS Collection Version C004												
All				0.30	0.23	0.42				0.41	0.18	0.497
Clear				0.24	0.26	0.17				0.198	0.27	0.07
Terra MODIS Collection Version C004												
All				0.22	0.31	0.35				0.21	0.28	0.33
Clear				0.54	0.10	0.59				0.48	0.16	0.52
Aqua MODIS Collection Version C005												
All				0.62	0.17	0.79	0.58	0.19	0.83	0.57	0.20	0.87
Clear				0.499	0.23	0.42	0.49	0.22	0.33	0.57	0.19	0.29
Terra MODIS Collection Version C005												
All				0.32	0.37	0.496	0.32	0.34	0.46	0.36	0.31	0.42
Clear				0.398	0.30	0.49	0.41	0.28	0.44	0.46	0.26	0.42
Aqua MODIS Deep Blue Algorithm												
All	1.25	-0.099	0.77	1.04	-0.02	0.79	0.85	0.05	0.81	0.69	0.09	0.80
Clear	1.64	-0.40	0.76	1.48	-0.31	0.79	1.37	-0.25	0.81	1.31	-0.19	0.798

Table 6.2: Values of parameters of correlation between various MODIS aerosol optical products and the Microtops sunphotometer derived aerosol optical depth during the Second ISRO GBP Land Campaign.

Chapter 7

Summary

Behaviour of three versions (Collection C004, C005 and Deep Blue algorithm) of MODIS aerosol product is studied over Ahmedabad, a semi-arid urban location in western India. Based on meteorology, the annual cycle is divided into Dry, Pre-Monsoon, Monsoon and Post-Monsoon seasons. Pre-Monsoon and Monsoon months are dominated by coarse mode aerosols whereas the Post-Monsoon and Dry months are charaterized by fine mode particles.

The Collection Version C004 of the MODIS aerosol product showed a large scatter in the correlation plot with the Microtops sunphotometer derived AOD values. The correlation plots were marked by slopes deviating from unity and large intercepts.

The updated MODIS aerosol product(C005) with better surface reflectance parameterization, updated aerosol models and other modifications to the retrieval procedure, shows a tremendous improvement in all the parameters of the correlation plot. In the validation results of MODIS aerosol product from Aqua platform, the intercepts for all years and all seasons are less than 0.05 at both 470 and 660 nm. Among all the years, 2005 shows the best correlation with R^2_{Blue} =0.71 and R^2_{Red}=0.75. $Slope_{Blue}$=0.78 and $Slope_{Red}$=0.90 are closest to unity and intercepts are lowest for this year as compared to other years- a feature related to the highest rainfall received during this year as compared to others which reduces the surface reflectance. Pre-Monsoon season shows the best correlation among all the seasons with

R^2_{Blue} =0.73, R^2_{Red}=0.81, $Slope_{Blue}$=0.84, $Slope_{Red}$=0.81, $Intercept_{Blue}$ = 0.01 and $Intercept_{Red}$ = -0.0005. Further, this season shows the maximum improvement in correlation from the C004 data which is attributed to the better parameterization of surface reflectance in the updated product which is usually high during this season.

Still, the updated product also has slope of correlation plots less than unity denoting need of further improvement in the aerosol model. It is also noted that the underestimation is large at 470 nm during Dry and Post-Monsoon months and at 670 nm during Pre-Monsoon and Monsoon months which implies that the aerosol model used by MODIS underestimates fine mode particle number during Dry and Post-Monsoon months and coarse mode particle number during Pre-Monsoon and Monsoon months.

Similar improvement in the retrieved aerosol optical depth values is noted in MODIS C005 data from Terra platform as well. Among years, 2004 has the slope closest to unity and overall good correlation. However, intercept of the correlation plot- denoting the errors due to surface reflectance, are lowest for 2005 in Terra C005 data as well. Monsoon month has overall good correlation and slopes closer to unity than other seasons whereas the intercepts of correlation plots are lowest during Post Monsoon season. The larger underestimation at 470 nm during Dry and Post Monsoon season is seen in this dataset also. Similary, the greater underestimation at 660 nm during Monsoon month, as observed in Aqua MODIS data, is seen in Terra C005 data as well. These features reinforce the need for further modification in the aerosol models used in the inversion algorithm. However, Pre Monsoon season which is also characterized by coarse particles and has larger underestimation at 660 nm in the Aqua MODIS C005 validation, has slopes nearly equal at 470 and 660 nm in the Terra MODIS C005 validation. This feature requires further examination.

Overall behaviour of the updated product is much better than collection version C004 especially in regard to surface reflectance related uncertainties. The errors related to the aerosol model uncertainties can be reduced with availability of more in-situ data.

Deep Blue algorithm, proposed as an alternative retrieval scheme in addi-

tion to the conventional procedure, shows promising for AOD retrieval over highly reflecting surfaces. Study of the aerosol product from this algorithm over Gujarat shows that the algorithm fills in the gaps over the Rann of Kuchh region over which the conventional MODIS algorithm is not able to make retrievals because of extremely high value of surface reflectance. However, examination of the aerosol product corresponding to this algorithm over Ahmedabad shows that correlation of updated aerosol product C005 is better than the Deep Blue algorithm.

Besides studying the variation in validation parameters on a temporal basis from Ahmedabad, studies have been done to observe the behaviour of these parameters under different surface and environmental conditions during the two ISRO-GBP Land Campaigns.

A considerable improvement in the correlation coefficient is seen with upgrade to the C005 algorithm in both the Terra as well as Aqua data for the first Land campaign. Further, it is seen that during the onward trip of the experiment, when the amount of coarse particles was less in the atmosphere, the underestimation was larger at blue, in accordance to the observation made in Ahmedabad studies. In addition, the Terra dataset showed larger underestimation at 660 nm during return leg of the campaign when the coarse mode particles increased in the atmosphere.

Validation carried out at Delhi as part of the Second ISRO GBP Land Campaign, showed a slight improvement in the Terra MODIS derived AOD with transition from C004 to C005 version. However, the improvement in the case of Aqua MODIS dataset was large. Clear sky data from both the platforms showed larger underestimation at blue wavelength as compared to red. During the season prevailing at the time of the experiment, the aerosol climatology is dominated by anthropogenic particles, so that this behaviour of slopes represents the inadequacy of the aerosol model used in the retrieval algorithm. The Deep Blue algorithm derived AOD values show good correlation with the sunphotometer values during this experiment.

Discussion of results by other groups

It is worthwhile to mention here the validation efforts at other locations by different groups and compare them with the results we have obtained. The major source providing the ground truth data for validation efforts elsewhere comes from the AERONET [Holben et al., 1998]. The procedure followed is the so called 'spatio-temporal approach' put forwarded by Ichoku et al. [2002]. There, the spatial average of MODIS derived AOD found from 50×50 km centred over the validation site is compared with the temporal average of AERONET AOD data taken within 1 hour of MODIS overpass. A further condition is imposed that there must be at least 5 pixels from MODIS data and 2 data points from AERONET for the validation to be valid.

The initial validation results of MODIS aerosol retrieval were provided by Chu et al. [2002] who used the 315 co-located measurements from AERONET sunphotometers and MODIS for the comparison. They found intercept of 0.06 and 0.02 at 470 and 660 nm respectively whereas the slope of the correlation plot was 0.86 at both the wavelengths. The correlation coefficient R at 470 and 660 nm was 0.91 and 0.85 respectively [Chu et al., 2002].

Ichoku et al. [2003] used the ground based observations of aerosol properties made during the SAFARI 2000 experiment to make an extensive investigation of behaviour of MODIS aerosol product especially in regard to the smoke aerosols produced as a result of biomass burning. They observed that during the biomass burning period, the AOT values predicted by MODIS were lower than AERONET especially at higher aerosol optical depth. They attributed this to the application of the same value of single scattering albedo(ω=0.90) for smoke aerosols globally and suggested lower values for southern African region [Ichoku et al., 2003]. This modification was implemented in the later version of the MODIS aerosol retrieval algorithm.

Chu et al. [2003] used collocated AERONET data and version 2 and version 3 MODIS aerosol data from August 2000 to July 2002 for the validation purpose thus encompassing a larger database of 3384 datapoint from worldwide observations. Their study revealed the slope of correlation plot to be 0.84 and 0.82 at 470 nm and 660 nm and intercepts to be 0.07 and 0.04 at

the aforesaid two wavelengths respectively. The correlation coefficient R was 0.91 and 0.82 respectively. These results were nearly similar to their earlier work [Chu et al., 2002]. In the same work, they reported the validation result of MODIS aerosol optical depth as compared against the handheld sunphotometer observation at Peking University, Beijing, China. In this case, they compared the sunphotometer measurements at 550 nm averaged over $\pm$ 1 hour of MODIS overpass against the MODIS derived AOD value within 10 km of the ground based observation site [Chu et al., 2003]. This comparison showed a slope of 0.86 and intercept of 0.08 with R value of 0.85.

Remer et al. [2005] used two years(August 2000 to August 2002) of Terra Collections 003 and 004 AOD data from MODIS to validate against the collocated AERONET aerosol optical depth values over land thus including 5906 data points representing approximately the data from all over the globe. Their validation effort showed a slope of 0.83 and 0.70 at 470 nm and 660 nm respectively. The intercepts at these two wavelengths were 0.09 and 0.059 whereas the corresponding R values were 0.83 and 0.68 respectively. They cite a possible calibration problem or improper representation of surface reflectance in some cases to be probable reasons for a positive bias seen at low optical thickness values.

Levy et al. [2005] carried out an extensive validation of the Level 2 MODIS aerosol product over both ocean as well as land during the CLAMS experiment of 2001 over the US east coast. This region had shown large discrepancy during the validation effort by Remer et al. [2005]. During this month long campaign(from 10 July 2001 to 2 August 2001), MODIS derived aerosol optical depth product was compared against a large database of ground based sunphotometers formed from AERONET, Microtops, LARC and AATS-14 sunphotometers. Their methodology was based on the spatio-temporal approach developed by Ichoku et al. [2002]. These comparisons revealed that although the MODIS retrievals were consistent with ground based data over oceans, there were substantial differences over land especially at blue wavelength. Only the validation results of aerosol optical depth over land are discussed here. Their results showed offsets of the correlation plots to be larger at 470 nm(0.26) as compared to that at 660 nm(0.17) but slopes were

closer to unity at 470 nm(0.76) than 660 nm(0.46). Further, correlation was also found to be better at blue(R2=0.5) than at red(R2=0.17). Corresponding values at green wavelength were intermediate to that for blue and red [Levy et al., 2005]. This was a detailed study in the sense that besides performing an exhaustive validation of MODIS aerosol products, Levy et al. [2005] also looked for possible sources of error and tried to perform corrections for the same. Thus, in order to take into account the errors arising due to possibility of inappropriate aerosol model, they changed the aerosol model to Dubovik et al. [2002] model instead of the Remer and Kaufman [1998] urban/industrial model used in the aerosol retrieval. Similarly, in order to look into the possibility of improper surface reflectance parameterization, they performed atmospheric correction using the CLAMS experiment data and used the resulting VIS/mid-IR surface reflectance ratios for modified AOD retrievals. Both these processes were followed separately in order to assess the individual impact due to each of them. In this way, they found that the aerosol model modification and surface reflectance update improved the slopes and intercepts respectively of the correlation plots. Their results and work has been discussed here in detail since it forms the starting point as well as the framework for the updated MODIS aerosol product(C005). Therefore, any results obtained from the validation of this product should be interpreted in this light.

During initial validation of the Deep Blue algorithm derived aerosol optical depth values with the AERONET sunphotometer values at Ilorin(Nigeria), Hsu et al. [2004] found the retrived AOD to fall within the 20% of the sunphotometer values. In the same work, validation at Solar Village (Saudi Arabia) showed that the retrieved values were generally within 20% of the sunphotometer AOD values. During the ACE-Asia campaign [Huebert et al., 2003], Deep Blue retrievals at Dunhuang, Yulin, Inner Mongolia and Dalanzadgad were found to be generally within 30% of the AERONET sunphotometer measured AOD values at these locations. Comparison at the Beijing AERONET site also showed Deep Blue algorithm derived AOD values to be within 20% of the AERONET values [Hsu et al., 2006].

Among the Indian context elsewhere, validation of MODIS derived AOD

has also been attempted by Tripathi et al. [2005]. Using MODIS Level 2 AOD data from collection 4 and AERONET data(interpolated at 550 nm) for 2004, they found an overestimation by MODIS during dust and an underestimation during non-dust seasons with slopes and intercepts in the two cases 2.46, -0.63 and 0.69, 0.12 respectively. The R^2 values in both the cases (0.72 and 0.71 respectively) were nearly same.

In the context of studying the aerosol properties and their variation along the Indo-Gangetic basin, Jethva et al. [2005] compared the monthly mean AOD at 550 nm computed from MODIS Level 3 daily gridded data with the AERONET sunphotometer derived monthly mean AOD values from Kanpur, India for the period January 2001 to July 2003. They found a systematic overestimation by MODIS during summer and an underestimation during winter [Jethva et al., 2005].

Prasad and Singh [2007] validated the MODIS monthly averaged Level 3 data against the Level 2 data from AERONET at 550 nm (interpolated from AERONET wavelengths) for a 4 year period from January 2001 to December 2004. They found MODIS overestimating the AOD values during summer and underestimating during winter with slope and intercept in the two cases 0.512, 0.5229 and 0.4843, 0.1522 respectively. The R^2 values in the two cases were 0.2937 and 0.4715 respectively [Prasad and Singh, 2007].

Results from validation of Collection Version C005 of the MODIS aerosol product have also started coming in from other groups as well. Li et al. [2007] examined Collection Version C004 and C005 of the MODIS aerosol product using hand held sunphotometers of the Chinese Sun Hazemeter Network over several locations encompassing different ecosystems. They find the slope of correlation plot to improve from 0.74 in the case of C004 to 0.98 for C005. Similar improvement is noticed in the intercept also which reduced from 0.179 in C004 comparison to 0.048 in C005. However, they find that both versions of the algorithm overestimate the aerosol optical depth over desert regions, and underestimate over forests. The retrievals are found to be more accurate over agricultural and suburban sites [Li et al., 2007].

Jethva et al. [2007] have studied the upgraded version over Kanpur (India) and found good correlation with the AERONET derived aerosol optical depth

values. They find the slopes of the correlation at 470, 550 and 660 nm to be $Slope_{470} = 0.92$, $Slope_{550} = 0.95$ and $Slope_{660} = 1.09$. Intercepts at the three wavelengths are $Intercept_{470} = 0.09$, $Intercept_{550} = 0.07$ and $Intercept_{660} = 0.05$ [Jethva et al., 2007].

Mi et al. [2007] made assessment of improvement in the AOD retrieval by MODIS with upgrade to C005 version at two AERONET sites Xianghe and Taihu in China. The slope of correlation at 550 nm for C004 aerosol product at Xianghe and Taihu were 0.70 and 0.892 respectively. The intercepts for these comparisons were 0.208 and 0.163 respectively. With upgrade to Collection Version C005, these parameters improved in the case of Xianghe to $Slope_{550} = 1.03$, $Intercept_{550} = 0.021$ and for Taihu to $Slope_{550} = 1.032$, $Intercept_{550} = 0.154$.

These points have been summarized in Table 7.1. One noticeable feature is the obvious dependence of the correlation on the study location. This highlights the importance of the detailed validation of MODIS aerosol product for different geographical regions. Another feature worth mentioning is the different values of the slopes and intercepts at different wavelengths, especially in Remer et al. [2005], Levy et al. [2005] and our work. Since the dominance of particles of a particular size is best reflected at a particular wavelength and also because of surface reflectance dependence on wavelengths, validation carried out at more than one wavelength provides more details regarding possible improvements to aerosol model, surface reflectance etc. Further, a classification of the correlation in terms of seasonal variation, as in our study, will reflect the precise cases where account of seasonal changes in the aerosol type and surface features are needed.

	Details of Study			Correlation Coefficients					
				470nm		550nm		660nm	
Group	**Ver**	**Lev**	**Location**	**Sl**	**In**	**Sl**	**In**	**Sl**	**In**
Chu et al [2002]		2	Global	0.86	0.06			0.86	0.02
Chu et al [2003]	2, 3	2	Global	0.84	0.07			0.82	0.04
Chu et al [2003b]	2, 3	2	Beijing			0.86	0.08		
Remer et al [2005]	3, 4	2	Global	0.83	0.09	0.78	0.068	0.7	0.059
Levy et al [2005]	4	2	US (EC)*	0.76	0.26	0.64	0.21	0.46	0.17
Tripathi et al	4	2	Knp(ND)*			0.69	0.12		
[2005]			Knp(D)			2.46	-0.63		
Prasad and Singh		3	Knp(S)*			0.51	0.52		
[2007]			Knp(W)			0.48	0.15		
Li et al. [2007]	4	2	China			0.74	0.179		
	5	2				0.98	0.048		
Jethva et al. [2007]	5	2	Knp*	0.92	0.09	0.95	0.07	1.09	0.05
Mi et al. [2007]	4	2	Xianghe			0.70	0.208		
	5	2				1.03	0.021		
	4	2	Taihu			0.892	0.163		
	5	2				1.032	0.154		
Present study[a]	4	2		0.51	0.15	0.52	0.18	0.65	0.18
(Aqua)	5	2		0.69	0.03	0.73	0.02	0.80	0.003
	DB	2	Ahmd*	0.73	-0.01	0.77	-0.02	0.91	-0.06
	4	2		0.54	0.16	0.57	0.18	0.76	0.16
(Terra)	5	2		0.57	0.10	0.60	0.08	0.73	0.04
Present study[b]	4	2		0.21	0.20			0.48	0.25
(Aqua)	5	2		0.295	0.13	0.30	0.12	0.35	0.11
	DB	2	LC1	0.74	-0.05	0.68	-0.03	0.65	-0.008
	4	2		0.66	0.03			0.54	0.20
(Terra)	5	2		0.76	-0.01	0.81	-0.02	0.94	-0.01
Present study[c]	4	2		0.30	0.23			0.41	0.18
(Aqua)	5	2		0.62	0.17	0.58	0.19	0.57	0.20
	DB	2	LC2	1.04	-0.02	0.85	0.05	0.69	0.09
	4	2		0.22	0.31			0.21	0.28
(Terra)	5	2		0.32	0.37	0.32	0.34	0.36	0.31

Table 7.1: A comparison of the validation results obtained by different groups quoted in this paper. Version and level of MODIS aerosol product, region of study and slope and intercepts at 470, 550, 660 nm are given. Kanpur (D) and Kanpur (ND) represent Dust and Non-Dust period for Kanpur respectively. Similarly Kanpur(S) and Kanpur(W) represent Summer and Winter period validation data over Kanpur. Two other studies by Ichoku et al [2003] and Jethva et al [2005] have not been shown since they do not quote coefficients of the correlation. Ichoku et al [2003] found underestimation by MODIS over Southern Africa attributed to insufficient absorption by MODIS aerosol model. Jethva et al [2005] found overestimation by MODIS during summer and underestimation during winter over Kanpur. *Knp = Kanpur, Ahmd = Ahmedabad, US(EC) = US East Coast

Bibliography

William L. Barnes, Thomas S. Pagano, and Vincent V. Salomonson. Prelaunch Characteristics of the Moderate Resolution Imaging Spectroradiometer (MODIS) on EOS-AM1. *IEEE Trans. Geosci. Rem. Sens.*, 36: 1088–1100, July 1998.

N. Bellouin, O. Boucher, J. Haywood, and M. S. Reddy. Global estimate of aerosol direct radiative forcing from satellite measurements. *Nature*, 438: 1138–1141, December 2005. doi: 10.1038/nature04348.

R. J. Charlson, S. E. Schwartz, J. M. Hales, R. D. Cess, J. A. Coakley, Jr., J. E. Hansen, and D. J. Hofmann. Climate Forcing by Anthropogenic Aerosols. *Science*, 255:423–430, January 1992.

D. A. Chu, Y. J. Kaufman, C. Ichoku, L. A. Remer, D. Tanré, and B. N. Holben. Validation of MODIS aerosol optical depth retrieval over land. *Geophys. Res. Lett.*, 29, June 2002.

D. A. Chu, Y. J. Kaufman, G. Zibordi, J. D. Chern, J. Mao, C. Li, and B. N. Holben. Global monitoring of air pollution over land from the Earth Observing System-Terra Moderate Resolution Imaging Spectroradiometer (MODIS). *J. Geophys. Res.*, 108, November 2003. doi: 10.1029/2002JD003179.

D. Allen Chu and Lorraine Remer. MODIS observation of aerosol loading from 2000 to 2004. *Earth Science Satellite Remote Sensing, Science and Instruments, Volume 1*, pages 92–110, 2006.

C. E. Chung, V. Ramanathan, D. Kim, and I. A. Podgorny. Global anthropogenic aerosol direct forcing derived from satellite and ground-based observations. *J. Geophys. Res.*, 110, December 2005. doi: 10.1029/2005JD006356.

G. A. D'Almeida, Peter Koepke, and Eric P. Shettle. *Atmospheric Aerosols: Global Climatology and Radiative Characteristics*. A. Deepak Publishing, 1991.

J. V. Dave. Intensity and polarization of the radiation emerging from a plane-parallel atmosphere containing monodispersed aerosols. *App. Opt.*, 9:2673–2684, 1970.

P. Y. Deschamps, F. M. Breón, M. Leroy, A. Podaire, A. Bricaud, J. C. Buriez, and G. Seźe. The POLDER mission: Instrument characteristics and scientific objectives. *IEEE Trans. Geosci. Rem. Sens.*, 32:598–615, 1994.

P. C. S. Devara, G. Pandithurai, P. E. Raj, and S. Sharma. Investigations of aerosol optical depth variations using spectroradiometer at an urban station, Pune, India. *J. Aerosol Sci.*, 27:621–632, 1996.

P. C. S. Devara, S. K. Saha, P. Ernest Raj, S. M. Sonbawne, K. K. Dani, Y. K. Tiwari, and R. S. Maheshkumar. A four-year climatology of total column tropical urban aerosol, ozone and water vapor distributions over Pune, India. *Aerosol and Air Quality Research*, 5:103–114, 2005.

O. Dubovik, B. Holben, T. F. Eck, A. Smirnov, Y. J. Kaufman, M. D. King, D. Tanré, and I. Slutsker. Variability of Absorption and Optical Properties of Key Aerosol Types Observed in Worldwide Locations. *J. Atmos. Sci.*, 59:590–608, February 2002.

D. P. Edwards, L. K. Emmons, D. A. Hauglustaine, D. A. Chu, J. C. Gille, Y. J. Kaufman, G. Pétron, L. N. Yurganov, L. Giglio, M. N. Deeter, V. Yudin, D. C. Ziskin, J. Warner, J.-F. Lamarque, G. L. Francis, S. P. Ho,

D. Mao, J. Chen, E. I. Grechko, and J. R. Drummond. Observations of carbon monoxide and aerosols from the Terra satellite: Northern Hemisphere variability. *J. Geophys. Res.*, 109, 2004. doi: 10.1029/2004JD004727.

K. F. Evans and G. L. Stephens. A new polarized atmospheric radiative transfer model. *J. Quant. Spec. and Rad. Trans.*, 46:413–423, November 1994.

K. F. Fraser and G. L. Stephens. A new polarized atmospheric radiative transfer model. *J. Quant. Spec. and Rad. Trans.*, 46:413–423, November 1994.

D. Ganguly, A. Jayaraman, and H. Gadhavi. Physical and optical properties of aerosols over an urban location in western India: Seasonal variabilities. *J. Geophys. Res.*, 111, December 2006a. doi: 10.1029/2006JD007392.

Dilip Ganguly, A. Jayaraman, T. A. Rajesh, and H. Gadhavi. Wintertime aerosol properties during foggy and nonfoggy days over urban center Delhi and their implications for shortwave radiative forcing. *J. Geophys. Res.*, 111, December 2006b. doi: 10.1029/2006JD007029.

Charles. K. Gatebe, Michael. D. King, Si-Chee. Tsay, Q. Ji, G. Thomas Arnold, and Jason Y. Li. Sensitivity of Off-Nadir Zenith Angles to Correlation between Visible and Near-Infrared Reflectance for Use in Remote Sensing of Aerosol over Land. *IEEE Trans. Geosci. Rem. Sens.*, 39:805–819, April 2001.

J. R. Herman and E. A. Celarier. Earth surface reflectivity climatology at 340-380 nm fro TOMS data. *J. Geophys. Res.*, 102:28003–28011, December 1997.

B. N. Holben, E. Vermote, Y. J. Kaufman, D. Tanré, and V. Kalb. Aerosols retrieval over land from AVHRR data - Application for atmospheric correction. *IEEE Trans. Geosci. Rem. Sens.*, 30:212–222, 1992.

B. N. Holben, T. F. Eck, I. Slutsker, D. Tanré, J. P. Buis, A. Setzer, E. Vermote, J. A. Reagan, Y. J. Kaufman, T. Nakajima, F. Lavenu, I. Jankowiak,

and A. Smirnov. AERONET- A federated instrument network and data archive for aerosol characterization. *Remote Sens. Environ.*, 66(1):1–16, 1998.

B. N. Holben, D. Tanré, A. Smirnov, T. F. Eck, I. Slutsker, N. Abuhassan, W. W. Newcomb, J. S. Schafer, B. Chatenet, F. Lavenu, Y. J. Kaufman, J. V. Castle, A. Setzer, B. Markham, D. Clark, R. Frouin, R. Halthore, A. Karneli, N. T. O'Neill, C. Pietras, R. T. Pinker, K. Voss, and G. Zibordi. An emerging ground-based aerosol climatology: Aerosol optical depth from AERONET. *J. Geophys. Res.*, 106:12067–12098, 2001. doi: 10.1029/2001JD900014.

N. Christina Hsu, Si-Chee. Tsay, Michael. D. King, and R. Hermans Jay. Aerosol Properties Over Bright-Reflecting Source Regions. *IEEE Trans. Geosci. Rem. Sens.*, 42:557–569, March 2004.

N. Christina Hsu, Si-Chee. Tsay, Michael. D. King, and R. Herman Jay. Deep Blue Retrievals of Asian Aerosol Properties During ACE-Asia. *IEEE Trans. Geosci. Rem. Sens.*, 44:3180–3195, March 2006.

Barry J. Huebert, Timothy Bates, Philip B. Russell, Guangyu Shi, Young Joon Kim, Kimitaka Kawamura, Greg Carmichael, and Teruyuki Nakajima. An overview of ACE-Asia: Strategies for quantifying the relationships between Asian aerosols and their climate impacts . *J. Geophys. Res.*, 108, 2003. doi: 10.1029/2003JD003550.

R. B. Husar, J. M. Prospero, and L. L. Stowe. Characterization of tropospheric aerosols over the oceans with the NOAA Advanced Very High Resolution Radiometer optical thickness operational product. *J. Geophys. Res.*, 102:16889–16909, 1997.

Keith D. Hutchison. Applications of MODIS satellite data and products for monitoring air quality in the state of Texas. *Atm. Env.*, 37:2403–2412, 2003.

Keith D. Hutchison, Solar Smith, and Shazia Faruqui. The use of MODIS data and aerosol products for air quality prediction. *Atm. Env.*, 38:5057–5070, 2004.

C. Ichoku, D. A. Chu, S. Mattoo, Y. J. Kaufman, L. A. Remer, D. Tanré, I. Slutsker, and B. N. Holben. A spatio-temporal approach for global validation and analysis of MODIS aerosol products. *Geophys. Res. Lett.*, 29, June 2002.

C. Ichoku, L. A. Remer, Y. J. Kaufman, R. Levy, D. A. Chu, D. Tanré, and B. N. Holben. MODIS observation of aerosols and estimation of aerosol radiative forcing over southern Africa during SAFARI 2000. *J. Geophys. Res.*, 108, April 2003. doi: 10.1029/2002JD002366.

A. Jayaraman, H. Gadhavi, D. Ganguly, A. Misra, S. Ramachandran, and T. A. Rajesh. Spatial variations in aerosol characteristics and regional radiative forcing over India: Measurements and modeling of 2004 road campaign experiment. *Atm. Env.*, 2006. doi: 10.1016/j.atmosenv.2006.01.034.

H. Jethva, S. K. Satheesh, and J. Srinivasan. Seasonal variability of aerosols over the Indo-Gangetic basin. *J. Geophys. Res.*, 110, November 2005. doi: 10.1029/2005JD005938.

H. S. Jethva, S. K. Satheesh, and J. Srinivasan. Assessment of second-generation MODIS aerosol retrieval (Collection 005) at Kanpur, India. *Geophys. Res. Lett.*, 34, 2007. doi: 10.1029/2007GL029647.

Menglin Jin, J. Marshall Shepherd, and Michael D. King. Urban aerosols and their variations with clouds and rainfall: A case study for New York and Houston. *J. Geophys. Res.*, 110, 2005. doi: 10.1029/2004JD005081.

Menas Kafatos and John J. Qu. Introduction to Science and Instruments. *Earth Science Satellite Remote Sensing, Science and Instruments, Volume 1*, pages 92–110, 2006.

Y. J. Kaufman and L. A. Remer. Detection of forests using mid-IR reflectance: An application for aerosol studies. *IEEE Trans. Geosci. Rem. Sens.*, 32:672–683, 1994.

Y. J. Kaufman, D. Tanré, L. A. Remer, E. F. Vermote, A. Chu, and B. N. Holben. Operational remote sensing of tropospheric aerosol over land from EOS moderate resolution imaging spectroradiometer. *J. Geophys. Res.*, 102:17051–17068, 1997a. doi: 10.1029/96JD03988.

Y. J. Kaufman, N. Gobron, B. Pinty, J.-L. Widlowski, and M. M. Verstraete. Relationship between surface reflectance in the visible and mid-IR used in MODIS aerosol algorithm - theory. *Geophys. Res. Lett.*, 29:31–1, December 2002a.

Y. J. Kaufman, D. Tanré, and O. Boucher. A satellite view of aerosols in the climate system. *Nature*, 419:215–223, September 2002b.

Y. J. Kaufman, O. Boucher, D. Tanré, M. Chin, L. A. Remer, and T. Takemura. Aerosol anthropogenic component estimated from satellite data. *Geophys. Res. Lett.*, 32, September 2005. doi: 10.1029/2005GL023125.

Yoram. J. Kaufman, Andrew. E. Wald, Lorraine. A. Remer, Bo-Cai Gao, Rong-Rong Li, and Luke Flynn. The MODIS 2.1 μm Channel- Correlation with Visible Reflectance for Use in Remote Sensing of Aerosol. *IEEE Trans. Geosci. Rem. Sens.*, 35:1286–1298, September 1997b.

M. D. King, Y. J. Kaufman, D. Tanré, and T. Nakajima. Remote Sensing of Tropospheric Aerosols from Space: Past, Present, and Future. *Bull. Am. Meteorol. Soc.*, 80:2229–2260, November 1999.

Michael. D. King, Yoram. J. Kaufman, W. Paul Menzel, and Didier Tanré. Remote Sensing of Cloud, Aerosol, and Water Vapor Properties from the Moderate Resolution Imaging Spectrometer (MODIS). *IEEE Trans. Geosci. Rem. Sens.*, 30:2–27, January 1992.

Michael. D. King, W. Paul Menzel, Yoram. J. Kaufman, Didier Tanré, Bo-Cai Gao, Steven Platnick, Steven A. Ackerman, Lorraine A. Remer, Robert

Pincus, and Paul A. Hubanks. Cloud and Aerosol Properties, Precipitable Water, and Profiles of Temperature and Water Vapor from MODIS. *IEEE Trans. Geosci. Rem. Sens.*, 41:442–458, February 2003.

R. B. A. Koelemeijer, J. F. de Haan, and P. Stammes. A database of spectral surface reflectivity in the range 335-772 nm derived from 5.5 years of GOME observations. *J. Geophys. Res.*, 108, 2003. doi: 10.1029/2002JD002429.

M. Leroy, J. L. Deuzé, F. M. Bréon, O. Hautecoeur, M. Herman, J. C. Buriez, D. Tanré, S. Bouffiès, P. Chazette, and J. L. Roujean. Retrieval of atmospheric properties and surface bidirectional reflectances over land from POLDER/ADEOS. *J. Geophys. Res.*, 102:17023–17038, 1997. doi: 10.1029/96JD02662.

R. C. Levy, L. A. Remer, J. V. Martins, Y. J. Kaufman, A. Plana-Fattori, J. Redemann, and B. Wenny. Evaluation of the MODIS Aerosol Retrievals over Ocean and Land during CLAMS. *J. Atmos. Sci.*, 62:974–992, April 2005.

R. C. Levy, L. A. Remer, and O. Dubovik. Global aerosol optical properties and application to Moderate Resolution Imaging Spectroradiometer aerosol retrieval over land. *J. Geophys. Res.*, 112, July 2007a. doi: 10.1029/2006JD007815.

R. C. Levy, L. A. Remer, S. Mattoo, E. F. Vermote, and Y. J. Kaufman. Second-generation operational algorithm: Retrieval of aerosol properties over land from inversion of Moderate Resolution Imaging Spectroradiometer spectral reflectance. *J. Geophys. Res.*, 112, July 2007b. doi: 10.1029/2006JD007811.

Robert. C. Levy, Lorraine. A. Remer, and Yoram. J. Kaufman. Effects of Neglecting Polarization on the MODIS Aerosol Retrieval Over Land. *IEEE Trans. Geosci. Rem. Sens.*, 42:2576–2583, November 2004.

Z. Li, F. Niu, K.-H. Lee, J. Xin, W.-M. Hao, B. Nordgren, Y. Wang, and P. Wang. Validation and understanding of Moderate Resolution Imaging

Spectroradiometer aerosol products (C5) using ground- bsed measurements from the handheld Sun photometer network in China. *J. Geophys. Res.*, 112, 2007. doi: 10.1029/2007JD008479.

K. N. Liou. *An Introduction to Atmospheric Radiation.* Academic Press, 2002.

W. Mi, Z. Li, X. Xia, B. Holben, R. Levy, F. Zhao, H. Chen, and M. Cribb. Evaluation of the Moderate Resolution Imaging Spectroradiometer aerosol products at two Aerosol Robotic Network stations in China. *J. Geophys. Res.*, 112, 2007.

Amit Misra, A. Jayaraman, and Dilip Ganguly. Validation of MODIS derived aerosol optical depth over western India. *J. Geophys. Res.*, 113, 2008. doi: 10.1029/2007JD009075.

M. Morys, Forrest M. Mims III, S. Hagerup, S. E. Anderson, A. Baker, J. Kia, and T. Walkup. Design, calibration, and performance of MICROTOPS II handheld ozone monitor and Sun photometer. *J. Geophys. Res.*, 106: 14573–14582, July 2001. doi: 10.1029/2001JD900103.

A. K. Prasad and R. P. Singh. Comparison of MISR-MODIS aerosol optical depth over the Indo-Gangetic basin during the winter and summer seasons(2000-2005). *Remote Sens. Environ.*, 107:109–119, 2007.

S. Ramachandran. Aerosol optical depth and fine mode fraction variations deduced from Moderate Resolution Imaging Spectroradiometer (MODIS) over four urban areas in India. *J. Geophys. Res.*, 112, 2007. doi: 10.1029/2007JD008500.

L. A. Remer and Y. J. Kaufman. Dynamic aerosol model: Urban/Industrial aerosol. *J. Geophys. Res.*, 103:13859–13871, 1998.

L. A. Remer, D. Tanré, Y. J. Kaufman, C. Ichoku, S. Mattoo, R. Levy, D. A. Chu, B. Holben, O. Dubovik, A. Smirnov, J. V. Martins, R.-R. Li, and Z. Ahmad. Validation of MODIS aerosol retrieval over ocean. *Geophys. Res. Lett.*, 29, June 2002.

L. A. Remer, Y. J. Kaufman, D. Tanré, S. Mattoo, D. A. Chu, J. V. Martins, R.-R. Li, C. Ichoku, R. C. Levy, R. G. Kleidman, T. F. Eck, E. Vermote, and B. N. Holben. The MODIS Aerosol Algorithm, Products, and Validation. *J. Atmos. Sci.*, 62:947–973, April 2005.

L. A. Remer, D. Tanré, Y. J. Kaufman, R. Levy, and S. Mattoo. Algorithm for remote sensing of tropospheric aerosol from MODIS: Collection 5. 39, November 2006.

Lorraine A. Remer, Andrew. E. Wald, and Yoram. J. Kaufman. Angular and Seasonal Variation of Spectral Surface Reflectance Ratios: Implications for the Remote Sensing of Aerosol Over Land. *IEEE Trans. Geosci. Rem. Sens.*, 39:275–283, February 2001.

John H. Seinfeld and Syros N. Pandis. *Atmospheric Chemistry and Physics: From Air Pollution to Climate Change.* Wiley-Interscience, 1997.

D. Tanré, Y. J. Kaufman, M. Herman, and S. Mattoo. Remote sensing of aerosol properties over oceans using the MODIS/EOS spectral radiances. *J. Geophys. Res.*, 102:16971–16988, 1997. doi: 10.1029/96JD03437.

O. Torres, P. K. Bhartia, J. R. Herman, Z. Ahmad, and J. Gleason. Derivation of aerosol properties from satellite measurements of backscattered ultraviolet radiation: Theoretical basis. *J. Geophys. Res.*, 103:17099–17110, 1998.

S. N. Tripathi, S. Dey, A. Chandel, S. Srivastava, R. P. Singh, and B. N. Holben. Comparison of MODIS and AERONET derived aerosol optical depth over the Ganga Basin, India. *Ann. Geophys.*, 23:1093–1101, June 2005.

E. F. Vermote, D. Tanré, J. L. Deuze, M. Herman, and J. J. Morcrette. Second Simulation of the satellite signal in the solar spectrum, 6S: An overview. *IEEE Trans. Geosci. Rem. Sens.*, 1997.

W. J. Wiscombe. Improved Mie scattering algorithms. *App. Opt.*, 33:1108–1110, 1994.

A. T. Young. Air mass and refraction. *App. Opt.*, 19:1505–1509, May 1980.

Publications in Refereed Journals

1. **Amit Misra**, A Jayaraman and Dilip Ganguly (2008), Validation of MODIS derived aerosol optical depth over western India, J. Geophys. Res., doi:10.1029/2007JD009075

2. Sanat Kumar Das, A Jayaraman and **A Misra** (2007), Fog induced variations in aerosol optical and physical properties over the Indo-Gangetic Basin and impact to aerosol radiative forcing, Annales Geophysicae (in Press)

3. A Jayaraman, H Gadhavi, D Ganguly, **A Misra**, S Ramachandran and T A Rajesh (2006), Spatial variations in aerosol characteristics and regional radiative forcing over India: Measurements and modeling of 2004 road campaign experiment, Atmospheric Environment, 40, 6504-6515

4. D Ganguly, H Gadhavi, A Jayaraman, T A Rajesh and **A Misra** (2005), Single scattering albedo of aerosols over the central India: Implications for the regional aerosol radiative forcing, Geophys. Res Lett., 32(L18803), doi: 10.1029/2005GL023903

Papers in Conferences/Symposia/Workshops

1. **Amit Misra** and A Jayaraman, A study on satellite retrieved aerosol optical depth over land, *XIII National Space Science Symposium*, 17-20 February 2004, Kottayam (India)

2. A Jayaraman, H Gadhavi, D Ganguly and **A Misra**, Lidar, sunphotometer and QCM studies of summertime variation in aerosol characteristics over Ahmedabad, *XIII National Space Science Symposium*, 17-20 February 2004, Kottayam (India)

3. **Amit Misra** and A Jayaraman, Phase Function dependence on relative humidity: Implications to satellite remote sensing, *IASTA meeting and*

International conference on Aerosol, Clouds and Indian Monsoon, 15-17 November 2004, Kanpur (India) **(Selected for the Best Poster Presentation Award).**

4. **Amit Misra**, Sanat Kumar Das and A Jayaraman, Study of aerosol properties during fog events from satellite and ground based observations, *4th Asian Aerosol Conference*, 13-16 December 2005, Mumbai (India)

5. **Amit Misra** and A Jayaraman, Study of environment with the aid of satellites, *National Symposium on Atmospheric and Environment Sciences- New Dimensions*, 19-20 January 2006, New Delhi (India) **(Selected for the Best Oral Presentation Award).**

6. **Amit Misra** and A Jayaraman, Study of MODIS derived AOD over Gangetic plain during winter 2004, *XIV National Space Science Symposium*, 9-12 February 2006, Vishakhapatnam (India)

7. **Amit Misra**, A Jayaraman and Dilip Ganguly, Accuracy of MODIS derived AOD over an urban location in western India, *SPIE Asia-Pacific Remote Sensing Symposium-2006*, 13-17 November 2006, Panaji (India)

8. **Amit Misra**, A Jayaraman and Dilip Ganguly, Study of seasonal variability in the MODIS AOD validation with ground truth data over Ahmedabad, *IASTA Conference on Emerging Trends in Aerosols: Technology and Applications*, 14-16 November 2007, New Delhi (India)

9. **Amit Misra**, A Jayaraman and Dilip Ganguly, Validation of MODIS aerosol product (Deep Blue Algorithm) over Ahmedabad, *International Symposium on Aerosol-Chemistry-Climate Interactions*, 20-22 November 2007, Ahmedabad (India)

10. **Amit Misra**, A Jayaraman and Dilip Ganguly, Study of MODIS aerosol product over Delhi during Second ISRO-GBP Land Campaign, *XV National Space Science Symposium*, 26-29 February 2008, Radio Astronomy Centre, Udhagamandalam (India)

11. **Amit Misra**, A Jayaraman and Dilip Ganguly, MODIS derived Aerosol Optical Depth over regions of high reflectance in Western India, *Asia Oceania Geosciences Society 5th Annual Meeting*, 16-20 June 2008, Busan (Korea)